Treatment of wastewater containing pharmaceutical compounds by catalytic wet peroxide oxidation using clay-based materials as catalysts

Adriano dos Santos Silva

Thesis report submitted to

Escola Superior de Tecnologia e Gestão

Instituto Politécnico de Bragança

Master Degree in

Chemical Engineering

Supervisors:

Prof. Helder Teixeira Gomes

Prof. Juliana Guerra Sgorlon

Dr. Jose Luis Díaz de Tuesta Triviño

Bragança

July, 2019

Treatment of wastewater containing pharmaceutical compounds by catalytic wet peroxide oxidation using clay-based materials as catalysts

Adriano dos Santos Silva

Thesis report submitted to **Escola Superior de Tecnologia e Gestão** of **Instituto Politécnico de Bragança** to obtain the Master Degree in **Chemical Engineering** in the ambit of the double diploma with the **Universidade Tecnológica Federal do Paraná - Câmpus Apucarana**

Supervisors:

Prof. Helder Teixeira Gomes

Prof. Juliana Guerra Sgorlon

Dr. Jose Luis Díaz de Tuesta Triviño

Bragança

July, 2019

ACKNOWLEDGEMENTS

First, I would like to thank God, for giving me the persistence to not give up on my goals. Because of this, I was able to have the courage needed to run after my dreams away from my family and out of my comfort zone.

Special thanks for those who always supported me, and always believed in me: my parents, Claudio and Ana, my brother Alessandro and my beloved girlfriend Camila Bertacco, my lifemate. You were the ones who gave me the strength that I needed to conclude this work.

Thanks to my supervisors, professor Dr. Helder Teixeira Gomes of Instituto Politécnico de Bragança (IPB) and professor Dr. Juliana Sgorlon Guerra of Universidade Tecnológica Federal do Paraná (UTFPR) for helping me with my work. I really appreciate the knowledge and trust given to me.

Special thanks to Dr. Jose Luis, for his help, lessons and for being by my side helping and doing everything that he could for the success of this work. Without you, I would take much longer to do everything that I needed. I also thank Me. Fernanda Roman for supporting me when Jose was too busy, I learned many things in the laboratory with you.

All my gratitude to my teachers from UTFPR – Apucarana and from IPB, that contributed to my personal and professional growth. To my friends from Apucarana (Brazil) and Bragança (Portugal) who were always by my side sharing moments of fun and learning that I will carry throughout my life.

To UTFPR and IPB institutions for giving me the opportunity to live this double degree. This experience made me grow professionally and even more personal. And last but not least, to VALORCOMP for the financial support and to LSRE-LCM for the opportunity to acquire knowledge in the catalysis field.

Abstract

This work deals with the treatment of wastewater containing paracetamol, used as a model pharmaceutical emergent pollutant, by catalytic wet peroxide oxidation using clay-based materials as catalysts. The catalysts prepared in this work were clays activated through acid treatment and clays pillared with Co and Fe. For the preparation, natural clays from four different regions of Kazakhstan were used: Akzhar, Asa, Karatau and Kokshetau. The FTIR analysis showed that the pillared clays have a higher amount of iron in its structure when compared with the natural materials, suggesting that the intercalation of iron was successful. The N_2 adsorption isotherms obtained were classified as Type II, typical of macroporous materials. The acid characterization showed that the procedures used for the preparation of the acid activated clays and of the pillared clays caused structural modifications. After the preparation and characterization, the pillared materials were tested in the degradation of paracetamol by catalytic wet peroxide oxidation (CWPO). Paracetamol concentration, hydrogen peroxide concentration and total organic carbon analysis (TOC) were followed against time. The material with the best activity was the Kokshetau pillared clay (KOP), with a complete conversion of the pollutant being obtained between 240 and 360 minutes of reaction, followed by a negligible iron leaching of 0.011 %. This leaching left the reaction system with a concentration of 0.089 mg/L of Fe, which is lower than the limit established by the European legislation for discharge in natural water courses (2 mg/L). Since the Kokshetau pillared clay presented the best result, other Kokshetau-based samples (activated, calcined and natural) were also tested in the CWPO of paracetamol. The higher efficiency of KOP in the CWPO of paracetamol can be explained by the fact that this material has a higher acidity, basicity and surface area when compared to the other pillared samples.

Keywords: Activated clays; Pillared clays; CWPO; Paracetamol; Contaminants of emerging concern.

Resumo

Este trabalho aborda o tratamento de águas residuais que contém paracetamol, como poluente emergente modelo, por oxidação humida com peróxido de hidrogênio usando argilas como catalisadores. Os catalisadores a base de argila preparados neste trabalho foram as argilas ativadas mediante tratamento com ácido e as argilas pilarizadas com Cobalto e Ferro. Para o preparo, foram utilizadas argilas naturais de quatro regiões diferentes no Cazaquistão: Akzhar, Asa, Karatau e Kokshetau. A análise de FTIR mostrou que as argilas pilarizadas possuem uma maior quantidade de Ferro na sua estrutura quando comparado com os outros materiais, o que pode indicar que o processo de intercalação do metal na estrutura da argila obteve sucesso. Os resultados obtidos para as isotermas de adsorção de N_2 foram usados para classificar o material como Tipo II, atribuída a materiais macroporoso. A caracterização ácida mostrou que os procedimentos usados para preparar a argila pilarizada e a argila ativada causaram modificações estruturais no material. Após a preparação e caracterização, as argilas pilarizadas foram testadas na degradação do paracetamol por meio da catálise húmida com peróxido de hidrogênio. A fim de avaliar a variação da concentração de paracetamol, peróxido de hidrogênio e a variação do teor de carbono orgânico total, amostras foram coletadas em diferentes tempos. O material com a melhor atividade foi a amostra de argila Kokshetau pilarizada (KOP), apresentando uma conversão completa do poluente entre 240 e 360 minutos de reação e uma quantidade de Ferro lixiviado de 0.011%. Essa porcentagem de lixiviação deixou o sistema reativo com uma concentração de Ferro de 0.089 mg/L, um valor menor que o valor limite estabelecido pela legislação (2 mg/L). Como entre as pilarizadas a amostra de Kokshetau demonstrou o melhor resultado, outras amostras a base de Kokshetau (ativada, calcinada e natural) também foram testadas na CWPO do paracetamol. O melhor desempenho da Kokshetau pilarizada pode ser justificado pelo fato de o material possuir uma maior quantidade de acidez, basicidade e área superficial com relação as outras argilas pilarizadas.

Palavras-chave: Argilas ativadas; Argilas pilarizadas; CWPO; Paracetamol; Contaminantes emergentes.

INDEX OF FIGURES

INDEX OF TABLES

INDEX OF ACRONYMS

AOP	Advanced oxidation process
CWPO	Catalytic wet peroxide oxidation
STP	Sewage treatment plant
NSAID	Nonsteroidal anti-inflammatory drug
UV	Ultraviolet
PILCs	Pillared clays
AKN	Akzhar natural
ASN	Asa natural
KAN	Karatau natural
KON	Kokshetau natural
AKA	Akzhar activated
ASA	Asa activated
KAA	Karatau activated
KOA	Kokshetau activated
AKC	Akzhar calcined
ASC	Asa calcined
KAC	Karatau calcined
KOC	Kokshetau calcined
AKP	Akzhar pillared
ASP	Asa pillared
KAP	Karatau pillared
KOP	Kokshetau pillared
FTIR	Fourier transformed infrared
IUPAC	International Union of Pure and Applied Chemistry
XRD	X-ray diffraction
HPLC	High performance liquid chromatography
TOC	Total organic carbon
pH_{PZC}	Point zero charge
MNP/CM	Magnetic nanoparticle/clay mineral

TABLE OF CONTENTS

INTRODUCTION

1 INTRODUCTION

In the last two hundred years, the population in the earth has been growing exponentially, as shown in Figure 1, reaching the mark of 7.53 billion people in 2017 [1]. As a result of this growth, the cities had the need to expand and to increase the occupation of the land surface, leading to a higher demand of primary resources (water, food, and electricity). The exponential growth of the population also increased the anthropogenic impact on the environment of the industries and generated the appearance of a different way to use the resources that are available [2].

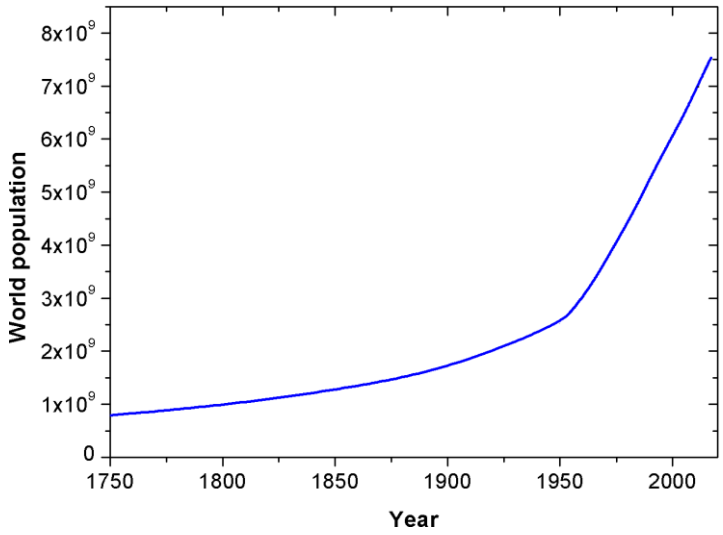

Figure 1. Evolution of the world population [1].

Although humans are passing through a slow learning procedure of how to deal with environmental issues, the search for different ways to establish a sustainable balance between the use of resources and the need of their preservation has increased in the past few years [2]. The concern with the survival of the future generations and the need to use resources that were not being used before has also made humans learn how to live in a changing environment [3].

Nowadays, global environmental pollution of various pharmaceuticals has become an environmental problem because of the increasing production and utilization of these products [4]. The risk of contamination and environmental pollution caused by drugs lies on the fact that they have high biological activity and ability to affect the metabolism of the living beings, even in small concentrations in the soil or in the water

[5]. In addition, the prolonged contact of drugs and pathogenic forms of bacteria in the environment significantly increases their resistance to drugs, reducing the efficiency of antibacterial agents used in the treatment of infectious diseases [6].

Among pharmaceutical compounds that can cause pollution of water, paracetamol (acetaminophen, 4-acetylaminophene-nol) deserves particular attention, since it has recently been discovered as a potential pollutant of waters [7–14]. Paracetamol is an analgesic and antipyretic drug that is largely accumulated in the aquatic environment due to its inefficient removal by conventional sewage treatment plants, also representing an important material for the industry of manufacture of azo dyes and photographic chemicals [15]. The concern about the environmental impact of its biodegradation products has been growing, because of its hepatotoxicity and the possibility of those products to be toxic or hazardous in trace amounts [8].

Among the possible treatments that can be used to degrade paracetamol existing in wastewaters, advanced oxidation processes (AOPs) are regarded as suitable options. Advanced oxidation processes are defined as those which involve the generation of hydroxyl radicals in sufficient quantity to affect water purification [16]. In 1987, when the concept of AOP was presented by William H. et. al., it was mentioned that the AOPs were treatments carried out with mild conditions, however, on later research works, AOPs have been explored in more severe temperature and pressure conditions, in order to ensure higher conversions. Nowadays, these treatments based on AOPs are very interesting, due to its efficiency for the degradation of soluble organic contaminants in water [17].

Catalytic wet peroxide oxidation (CWPO) is an AOP recognized as a low-cost technology by the fact that it operates under mild conditions (from ambient temperature to 140 °C and typically from atmospheric pressure until 10 bar) [18]. In the CWPO process, hydrogen peroxide (H_2O_2) acts as an oxidant and a suitable catalyst is used to decompose the molecules of H_2O_2 into hydroxyl and hydroperoxyl radicals ($HO^{\bullet}$ and $HOO^{\bullet}$). Hydroxyl radicals are highly oxidizing species, being able to efficiently degrade the organic pollutants present in water. The use of H_2O_2 as a source of hydroxyl radicals is environmentally-friendly because it is well-known that its total decomposition products are oxygen and water. That makes the CWPO-based water treatment further attractive from a sustainable point of view [18,19].

Clays have been explored for several applications as low-cost materials, showing interesting catalytic properties [20–23]. In the last years, studies about layered

aluminosilicate (clays) based materials report its high catalytic activity in the Fenton process used in the oxidation of organic pollutants. The clay-based materials have a low price and, depending on their preparation, present high stability to leach out metal ions into the aqueous solution. This fact coupled with the environmental safety of their utilization makes them well suited for application in water treatment processes [5, 6].

This dissertation work deals with the preparation of clay-based materials to be used as a catalyst in the CWPO process for the removal of paracetamol from aqueous solutions, used as model pharmaceutical wastewater. The raw materials considered in the preparation of the catalysts are 4 different natural clays extracted from Asa, Karatau, Kokshetau and Akzhar deposits in Khazakstan. This work proposes the production of a variety of clay-based materials, such as acid activated clays and pillared clays in order to evaluate and screen their catalytic activity to remove paracetamol from aqueous solution by CWPO.

STATE OF THE ART

2 STATE OF THE ART

2.1 CONTAMINATED WATERS

Water is the most essential substance for the human being to be able to maintain life and good health. However, the total amount of water available for human use is limited, and in the past few years problems related to pollutants are becoming more common and have been a constant public concern [24,25]. In the last decades, a new significant class of water pollutants have emerged, the pharmaceuticals and personal care products. As an example, recent analysis made in effluents has shown the presence of significant amounts of pharmaceutical drugs, not only in effluents arising from pharmaceutical industries, but also in surface and ground waters, and even in drinking waters [17,18].

The conventional pathway of pharmaceuticals into water is their release into the raw sewage, by excretions of humans (who excrete between 58 and 68% of the amount of pharmaceuticals that they have consumed) and also by some inefficient treatments in sewage treatments plants (STPs) and discharges into receiving waters, as illustrated in Figure 2 [9,19]. Most of the treatments applied to polluted waters with pharmaceuticals are inefficient in the removal of these compounds, which makes that some compounds as Ibuprofen and Diclofenac started being detected in aqueous samples worldwide [26]. In addition, the continuous input of pharmaceuticals into the aquatic environment, due to their usual persistence, represents a long-term risk to the aquatic environment [20,21].

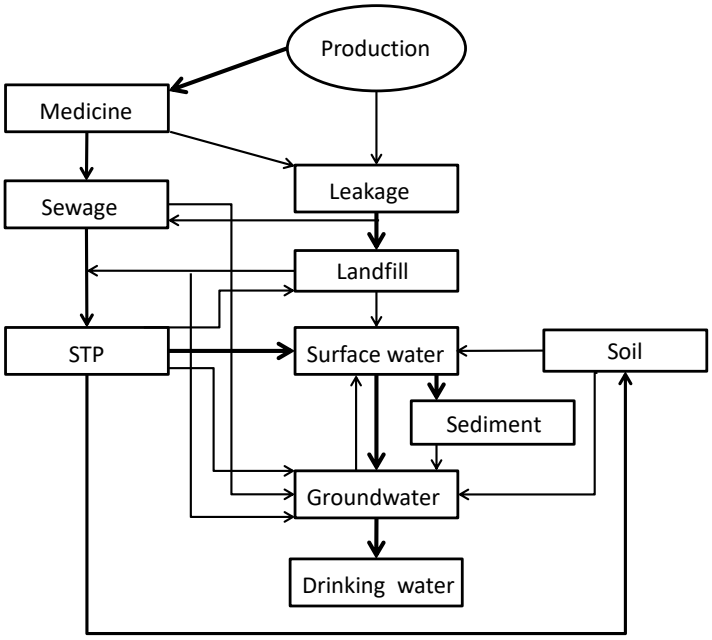

Figure 2. Pathway of the pharmaceuticals into aquatic systems [27] (modified from literature). STP= sewage treatment plants.

The presence of pharmaceutical contaminants in water, even at low concentration, could bring about harmful toxicological consequences to human beings and to animals that could ingest the contaminated water [28]. Compared with conventional pollutants, as phenolic compounds and chlorinated derivates, many pharmaceuticals possess water solubility, and most of them distribute and migrate in the environment by the aqueous phase transfer and food chain diffusion. Particularly, paracetamol (acetaminophen drug) is frequently detected in rivers, lakes, and groundwaters. For this reason, a lot of effort from the scientific community has been given in order to search new wastewater treatment technologies that can completely degrade paracetamol present in water [29].

Paracetamol (N-acetyl-para-aminophenol or para-acetyl-amino-phenol, also known as acetaminophen) is a nonsteroidal anti-inflammatory drug (NSAID) included in the top 200 prescriptions overall the world, commonly used to relieve the tension headache, muscular aches, general pain and rheumatic pain [24,30]. As paracetamol is a medicine very consumed by humans, its introduction in the aquatic environment by consumer use is continuous, and has increased in the past few years. There are some factors that contribute to the dangerous nature of paracetamol in the aquatic environment, as for example its solubility of 14 g/L in water at room temperature, and

Henry's constant of $6.42x10^{-11}$ $atm.m^3.mol^{-1}$, which indicates that it is present in the aqueous solution phase of surface waters with the possibility to migrate into groundwaters [25,31]. Since paracetamol is an organic pollutant, conventional treatments are not able to remove it from water. Despite of that, one alternative for the removal of such contaminant from the water is to use an advanced oxidation process. Figure 3 illustrates the molecule of paracetamol.

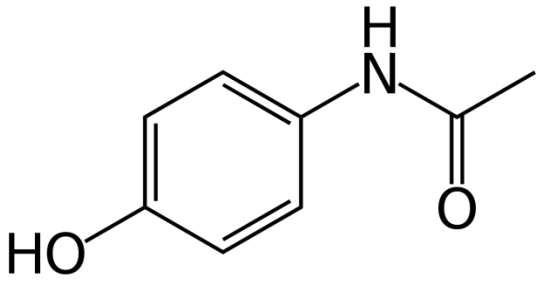

Figure 3. Paracetamol

2.2 ADVANCED OXIDATION PROCESSES

Wastewaters containing high concentrations of toxic and nonbiodegradable organic compounds are very hard to treat with conventional methods [9]. Many techniques such as adsorption, membrane filtration and flotation can only transfer the pollutants from one phase to another. In contrast, advanced oxidation processes (AOPs) can degrade and mineralize effectively various persistent organic compounds. These treatments can be used to minimize the discharge of organic pollutants into the receiving waters, being able to improve the overall quality status of secondary effluents for possible reuse [32]. In this scenario, the update of advanced treatment technologies has arisen as practice for the total decomposition of organic pollutants, by total mineralization or conversion into less harmful compounds [33].

AOPs are considered clean technologies for the treatment of polluted waters, in which hydroxyl radicals ($HO^{\bullet}$) are produced to oxidize the organic matter contained in wastewater effluents. The efficiency of AOPs is based on the generation of these highly reactive radicals, which are powerful oxidizing species. The radicals generated during the process are able to degrade indiscriminately organic pollutants, yielding CO_2, H_2O and inorganic ions [28,34]. The procedure can also completely degrade the organic compounds (mineralization), which represents the best scenario of the AOP process

since in this situation critical secondary wastes are not generated and there is no necessity to accomplish a post-treatment due to the absence of pollutants [35]. The combination of different AOPs in a sequence of complementary processes is also very employed to achieve a biodegradable effluent that can be treated by a cheaper conventional biological process.

AOPs includes several technologies to treat water, and they can implement ultraviolet (UV) radiation, ozone (O_3), hydrogen peroxide (H_2O_2) and oxygen (O_2). Some of the most studied and recognized AOPs are the Fenton and the Fenton-like processes [36]. Catalytic oxidation with hydrogen peroxide in aqueous solutions (Fenton or CWPO - catalytic wet peroxide oxidation) is an AOP involving the generation of highly active hydroxyl radicals through the decomposition of hydrogen peroxide in the presence of a suitable catalyst. Despite that hydrogen peroxide is a costly reactant in the CWPO process, its use is globally better than the processes that involve the use of gaseous oxygen. One factor that defines the efficiency of the oxidation process is the resistance to the mass transfer in the boundary, which in the case of hydrogen peroxide is very low, allowing the oxidizing reagent to act as a free-radical initiator, providing $HO^{\bullet}$ radicals that promote the degradation of the organic compounds [36].

2.2.1 Fenton

The Fenton process was discovered more than one hundred years ago by Henry J. Fenton. The scientist reported in his article that hydrogen peroxide could be activated by iron salts in order to oxidize tartaric acid. Despite of that, the process was only used for the first time for the removal of organic pollutants in the 1960s [10]. The interest of researchers around the world for this classic reactive system began around 1990 when some articles reported results obtained with the use of the Fenton process in the treatment of wastewater, and the interest in this field of study continues nowadays since the number of investigations on this application is still rising considerably [32,33].

The mechanism of the Fenton process is based on the generation of hydroxyl radicals from the decomposition of hydrogen peroxide in the presence of ferrous iron (Fe^{2+}) at acid conditions, yielding Fe^{3+} with the formation of hydroxide ions (OH^-) and hydroxyl radicals $HO^{\bullet}$ (Eq. 1). In the sequence of the reaction cycle, the ferric ion generated by oxidation in the first reaction reacts with hydrogen peroxide producing hydroperoxyl radicals and regenerating the catalyst, as described in Eq. 2. The

hydroperoxyl radical also reacts with the ferric ion, regenerating more catalyst (Eq. 3) [13,33,35].

$$H_2O_2 + Fe^{2+} \rightarrow Fe^{3+} + HO^{\bullet} + OH^{-} \quad (1)$$

$$Fe^{3+} + H_2O_2 \rightarrow Fe^{2+} + HOO^{\bullet} + H^{+} \quad (2)$$

$$Fe^{3+} + HOO^{\bullet} \rightarrow O_2 + H^{+} + Fe^{2+} \quad (3)$$

Despite the reactions described above, the process is much more complex and includes many other reactions [37]. In the last few years, the scientific community placed an increased effort in the development of heterogeneous catalysts that could avoid the formation of iron sludge, which complicates the discharge of the effluent resultant from the Fenton treatment, since the amount of iron sludge is not appropriate for reutilization [36,38]. The goal of the treatment of wastewaters by Fenton oxidation is to accomplish the almost complete degradation of the organic pollutants, trying to simultaneously to avoid the formation of undesirable compounds that would complicate even more the discharge of the wastewaters. The oxidation of the organic pollutants produces intermediate species, which can be oxidized to CO_2, H_2O and inorganic salts [39]. The overall process that involves the treatment of wastewater by Fenton can be described by Eqs. (4) and (5).

$$\textit{Pollutants} + H_2O_2 \xrightarrow{Fe^{2+}/Fe^{3+}} \textit{Intermediates} \quad (4)$$

$$\textit{Intermediates} + H_2O_2 \xrightarrow{Fe^{2+}/Fe^{3+}} CO_2 + H_2O_2 + \textit{inorganic salts} \quad (5)$$

2.2.2 Catalytic wet peroxide oxidation

In CWPO, H_2O_2 is employed as an oxidant and a heterogeneous catalyst is used to promote the decomposition of H_2O_2 to hydroxyl radicals, vital species to the successful implementation of CWPO. As explained before, hydroxyl radicals are highly oxidizing species, able to degrade most of the organic pollutants, and the H_2O_2 used to produce these radicals is well established as an environmentally friendly agent since its total decomposition products are oxygen and water [40,41].

The typical heterogeneous catalysts employed in CWPO processes consists on an active phase, some transition metal like Fe, supported on a material with high

porosity and surface area [42]. The use of supported catalysts allows the increasing of the surface area that provides the metal species. Alumina, silica, activated carbons, and clays are some possible materials that can be employed as catalyst supports. Despite the advantages of CWPO, its application to wastewater treatments has been restricted, since most of the catalysts have shown moderate activity and low stability, with metal leaching occurring into solution [43,44].

A fundamental study field of the CWPO process is the catalyst support typically used. Some of the materials that appear in the literature as catalyst supports include zeolites, silica, alumina and clays [25,37,39,40]. In the case of clays, it has been studied that its modification to pillared clays have emerged as a promising technique because it allows the production of materials with high resistance and thermal stability, increased porosity, surface area and basal spacing [23]. The combination of these properties of pillared clays with their low cost and environmental safety makes them promising for applications in water treatment processes [39]. As an example, the use of CWPO in the presence of pillared clays to treat organic wastewaters containing phenol is one of the most promising methods that has been studied in recent years [45,46].

Among the problems that usually appear in CWPO, metal leaching of the metallic phase to the reaction medium is that one being more studied [47,48]. This led to the study of different methods to synthetize metal-free materials, capable to catalyze the decomposition of H_2O_2 [49]. A class of materials that has attracted attention from the scientific community are metal-free catalysts, for example, activated carbons, which were found to be active catalysts for the CWPO of organic pollutants without any supported phase [42].

The development of metal-free catalysts for the CWPO process is of great interest since these materials are able to prevent iron leaching, deactivation and the use of high-cost metals. The possibility to synthetize a metal-free catalyst for CWPO of organic pollutants represent an advantage in comparison with the Fenton process, once that the use of these materials does not result in the formation of iron sludge, as occurs in Fenton [47]. In the studies regarding the use of metal-free catalysts in CWPO, moderate or low activities are in general reported for the removal of organic compounds, even when using doses of H_2O_2 higher than the stoichiometric [50–52]. On the other hand, clay-based materials present a higher activity for the removal of organic pollutants, which makes promising its use in CWPO of effluents containing pharmaceutical compounds [23,39,53].

2.3 CLAYS AND CLAY MINERALS

Clays are known by humans since a long time ago. The first indication of the use of clays minerals has been registered in the antiquity when homo erectus and homo neanderthalensis used ochers mixed with water and different types of mud to cure the wounds they had to clean their skin. Along with the history of mankind, several historical characters studied the uses of clays, most of them looking for the mineral benefits to human health. Aristotle referenced the deliberate consumption of clays by humans for therapeutic purposes. Marco Polo related that Muslim pilgrims ingested clays to cure fever, and this practice is still used in certain countries. From the antiquity until these days, clays have been used for many applications, as for example in pharmaceutical formulations and topical applications [54].

Despite the ancient roots on the use of mineral clays, the study of these materials from a scientific point view is recent. The concept of clay mineral began to be built in the mid of 1930s [55]. After that, a huge quantity of information about clays and clay minerals started appearing in the textbooks, in which was related to the structure, their modifications, and their applications. The classification of the clay minerals is based, commonly, on the planar hydrous phyllosilicates, as represented in Figure 4.

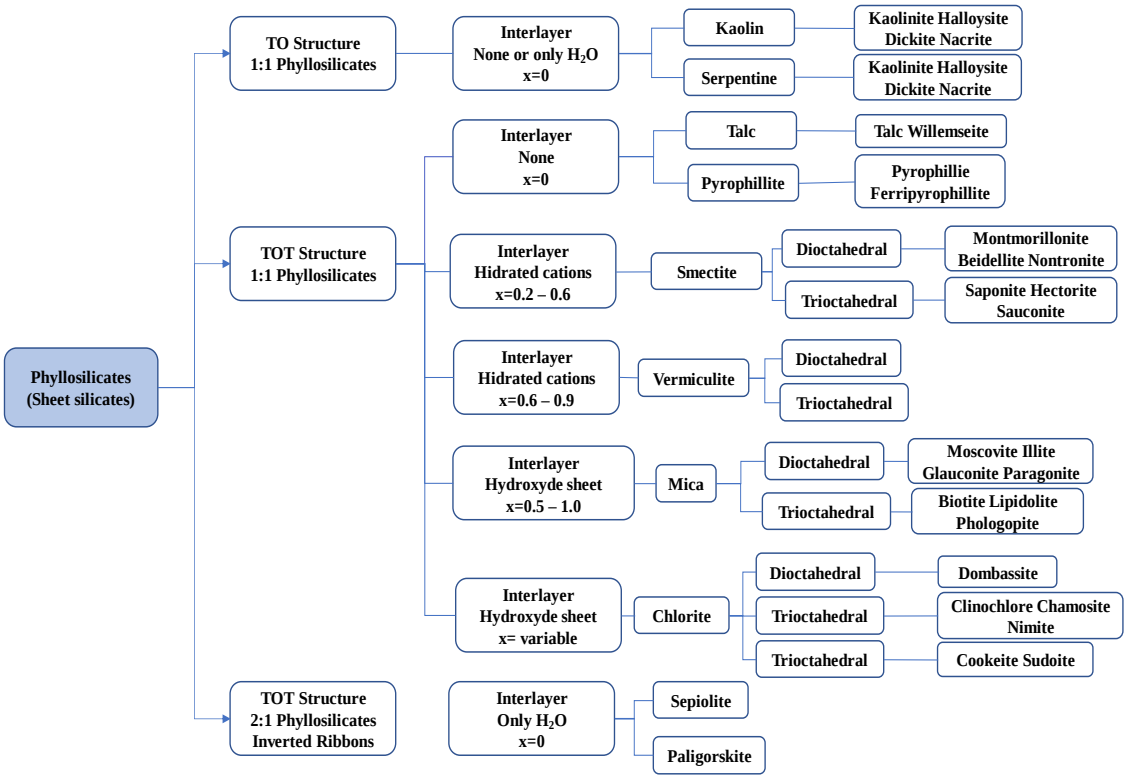

Figure 4. Classification of the phyllosilicates [56] (modified from literature).

An important group of natural clays that is not present in Figure 4 is bentonite. This occurs by the fact that bentonite is not a mineral, but a type of clay composed mostly by smectite minerals (such as montmorillonite) and minor concentration of zeolite and quartz [24].

The phyllosilicates, or sheet silicates, are an important group of minerals. The basic structure of the phyllosilicates is based on interconnected six-member rings of SiO_4^{4-} tetrahedra that pass out on endless sheets. Most part of the phyllosilicates contains hydroxyl ions, OH^-, in the center of the structure, which allows the formation of an octahedral structure that possesses a cation bonded to the hydroxyl ion. This connection between the hydroxyl ion and the cations form a layer in which appear the cations Fe^{2+}, Mg^{2+} or Al^{3+} [56]. The representation of the tetrahedral and octahedral sheets that composes the mineral clays is given in Figure 5.

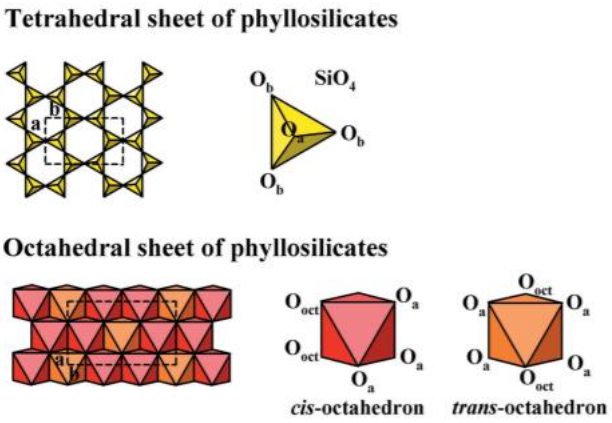

Figure 5. Tetrahedral and octahedral sheets [56].

A continuous tetrahedral sheet (T) usually formed by $[MO_4]^{4-}$ species, where M are the ions Fe^{2+}, Mg^{2+} or Al^{3+}. This structure is placed in the center of the tetrahedron in which there are four oxygen atoms located in the edges. The tetrahedron is linked to the adjacent structure by sharing three corners, resulting in a bidimensional pattern with hexagonal structure along the a, b plane (Figure 5) [57]. In Figure 6 it is possible to observe some examples of phyllosilicate sheets formed by TO and TOT structure.

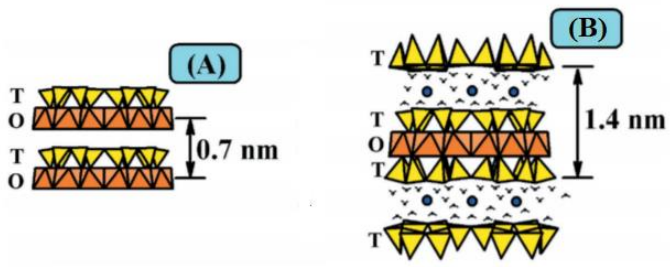

Figure 6. Structure of phyllosilicates. (A) Kaolin and serpentine, (B) Smectite [56]. (modified from literature).

The octahedra are connected by sharing edges, causing sheets with hexagonal symmetry and the repetition of a tetrahedral sheet (T) and an octahedral sheet (O) forms the phyllosilicates with TO structure (Figure 6A). This structure is typical of the clay minerals coming from kaolin and serpentine groups, which possess a basal spacing of 0.7 nm. The second formation of the phyllosilicates is the TOT structure (Figure 6B). In that structure, an octahedral sheet stays between two tetrahedral sheets faced to each other, obtaining minerals as smectite, with a basal spacing of 1.4 nm. The TO structure

is neutrally charged, meaning that the structure does not need cations to counter-balance the charge. On the other hand, the TOT structure in Figure 6B is not neutrally charged. Actually, this structure is generated by the excess of negative charges in the layer, which can be resulted from the exchange of the trivalent cations by divalent cations on the octahedral sheet [56].

The substitution of Si^{4+} species by the cations M^{3+} in the tetrahedral sheet generates an unbalance of charges in the basal and apical oxygens, leaving the conformation with a negative charge and affecting the organization of the TOT. In the same way that tetrahedral sheets can suffer modification in its structures caused by the substitution of Si^{4+} groups by M^{3+}, the octahedral structures can be modified by divalent cations, generating an excess of negative charge in the layer. The different groups of TOT are determined by the layer charge. While the smectite group is featured by charges in the range of 0.2 to 0.6 per unit cell, the vermiculite groups are featured by layers with charges between 0.6 and 0.9 per unit cell. The other classifications of phyllosilicates are not relevant for this work [58].

2.4 DEVELOPMENT OF CLAY-BASED MATERIALS

2.4.1 Pillared clays

Pillared clays (PILCs) are porous materials resulting from the process of pillaring lamellar clays. The preparation of pillared clays is one approach to the rational design of porous solids with a pore size distribution on a molecular length scale. Pillared clays are a special class of intercalated compounds in which the intercalant gallery is sufficiently large to allow access to the intracrystal surfaces of the layered structure [57]. Their high surface area and permanent porosity allow them to be very attractive solids for adsorption and catalysis purposes [59]. Thus, the research interest in these materials has increased considerably in the last few years.

PILCs can be obtained from smectite clay minerals through a procedure that can be divided into three fundamental steps: a) preparation of the pillaring solution that contains the pillaring cations (as for example Al^{3+}, Ga^{3+}, Ti^{4+}, Zr^{4+}, Fe^{3+} and Cr^{3+}); b) intercalation of these cations into the interlayer space of the clays, which involves the natural substitution of exchangeable cations present between the sheets of the clay mineral; and c) calcination of the filtered material under moderate conditions. The last

step is essential to the formation of the pillared clays, since with the calcination the polycations present in the clay are transformed into stable oxi-hydroxides named pillars, and the solid obtained after this procedure is called pillared clay [60]. In Figure 7 it is possible to observe more visually how the process of pillaring occurs.

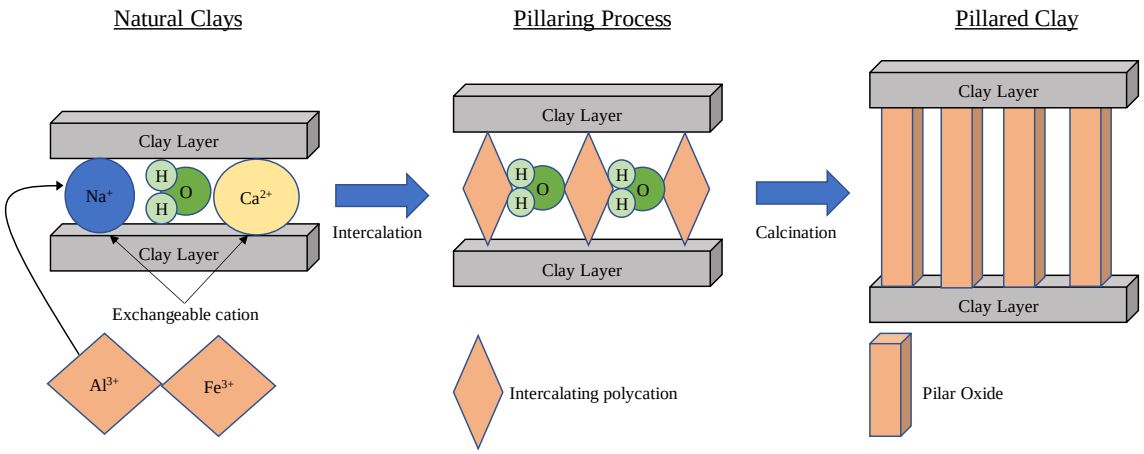

Figure 7. Representation of the pillaring process [23] (modified from literature).

A great variety of factors can influence the pillaring process, such as the chemical composition of the clay, its crystallinity, nature, and contents of exchangeable cations and impurities (e.g. quartz) [61].

Many research studies describe methods to pillar montmorillonites and bentonites, which are the mostly used clays [22,39,62]. The first step to pillar the clay is to prepare a clay colloid. For this, a 0.5 – 2.5 wt.% clay colloid is normally prepared by dispersing the clay in water under prolonged stirring. In order to facilitate the exchange of the cations present in the structure of the clay by the cations present in the pillaring solution, it is possible to insert Na^+, for example, with the procedure described by Khalaf [63]. The insertion of the sodium cation leaves the natural clay with uniform composition and, in addition, increasing its CEC and thermal stability [64,65]. The intercalating solution is very important for the pillaring process since this solution contains the cation(s) that will substitute the original cations of the clay. The pillaring cations, the clays and the conditions used in some works are described in Table 1.

Table 1. Pillaring cations and pillaring conditions employed to pillar clays.

References	Pillaring cations	Clays	Pillaring Time (h)	Pillaring Temperature (°C)
53	Al^{3+}, Cu^{2+}	Bentonite	48	40
53	Al^{3+}, Fe^{3+}	Bentonite	48	40
63	Al^{3+}	Bentonite	48	40
66	Al^{3+}	Bentonite	5	69
67	Al^{3+}, Ga^{3+}	Montmorillonite	24	50
68	Al^{3+}	Montmorillonite	2	25
68	Zr^{4+}	Montmorillonite	8	25
69	Al^{3+}, Cr^{3+}	Montmorillonite	4	70
39	Al^{3+}, Cu^{2+}, Fe^{3+}	Montmorillonite	24	* N. M
70	Al^{3+}, Zr^{4+}	Montmorillonite	24	25
41	Al^{3+}	Montmorillonite	24	80

***N.M. = Not mentioned**

Analyzing the different conditions presented in Table 1, it is possible to observe that the cations used for the pillaring solution are bigger than the cations present in the structure of the natural clays (*e.g.* Ca^{2+} and Na^{+}). In fact, the choice of Al^{3+} as an exchangeable cation occurs in most of the works, and this is because the pillaring solution of this cation is easier to prepare, showing this cation good results [41,63,66]. Temperature is also an important parameter for the pillaring process, and as it's possible to observe in Table 1, the temperatures are also lower than 100°C, since high temperatures can disturb the process of exchange of the cations. The problem with high temperatures during the process of exchange is that the shaking of the system (caused by high temperatures) makes difficult the pillaring cation to reach the sheets of the phyllosilicates, where are the exchangeable cations [71].

2.4.2 Acid activated clays

The acid activation of the clay consists on the reaction between the clay mineral with an acid solution, such as sulfuric, nitric or phosphoric acids. The procedure is broadly used in the cleaning (washing) of natural clays, or even in order to increase the surface area of the clay [72]. During the decomposition stage, the octahedral cations are released from the layered structure, creating Lewis and Brönsted sites, which increases the catalytic potential of these materials [73]. The mechanism consists of an acid attack, in

which the hydrated cations present in the interlayer spaces of the clay mineral are exchanged by hydrated protons. In Figure 8 there is an illustration of the formation of an acid activated montmorillonite.

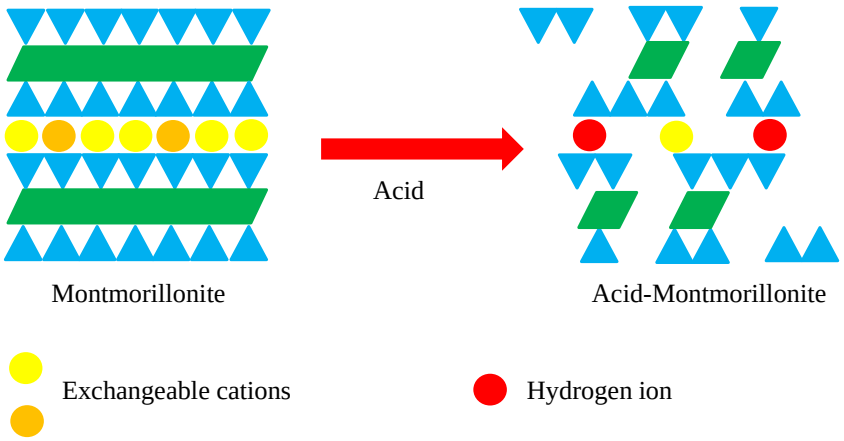

Figure 8. Scheme of the acid activated montmorillonite formation [74].

Table 2 summarizes the optimal operating conditions employed in different studies related to the acid activation of different clays.

Table 2. Studies related with acid activated clays.

References	Acid	Conc.	Time (min)	Temp. (°C)	S_{BET} (m^2/g) Before	S_{BET} (m^2/g) After	Solid /Liquid
75	HNO_3	3 M	45	* N. M	32	53	1:4
75	HNO_3	4 M	45	* N. M	32	101	1:4
76	H_2SO_4	30%	2400	80	10	30	1:4
76	H_2SO_4	40%	2400	80	10	14	1:4
77	H_3PO_4	1 M	180	100	50	91	1:4
77	H_3PO_4	1 M	240	100	50	95	1:4
77	H_3PO_4	2 M	180	100	50	140	1:4
77	H_3PO_4	2 M	240	100	50	112	1:4
77	H_3PO_4	4 M	180	100	50	182	1:4
77	H_3PO_4	4 M	240	100	50	174	1:4
74	HCl	10%	480	40	20	203	1:62.5
78	HCl	6 M	120	90	115	307	1:10
79	HNO_3	4 M	360	50	63	99	1:30
80	HCl	3 M	120	90	96	220	1:4
80	HCl	4.5 M	120	90	96	253	1:4
81	H_2SO_4	1 M	120	80	65	92	1:10
81	H_2SO_4	4 M	120	80	65	134	1:10
82	H_2SO_4	5 M	240	110	23	107	* N. M
82	H_2SO_4	10 M	240	110	23	143	* N. M

***N.M. = Not mentioned**

As can be observed the surface area increased in all cases after acid activation. Some of the studies presented in Table 2 have done a comparison between the change of some parameters. For example, Wehrs et al. [71] have shown that using HNO_3 with a concentration of 4 M is better than with a concentration of 3 M under the same time and temperature conditions. This behavior was also observed by Mache et. al. [81] and Panda et. al. [82] when the increase of the surface area of the resultant material was associated with an increase in the concentration of H_2SO_4 used in acid activation.

Time is another crucial parameter in the acid activation procedure. For that Zatta et. al. [77] showed that an increase in the time of acid activation also increased the surface area, for the case when H_3PO_4 was used. The temperature and the solid/liquid ratio, in most of the studies, were parameters maintained constant.

2.4.3 Applications of modified clays

2.4.3.1 CWPO of pharmaceuticals with pillared clays

Processes of the pharmaceutical industry generate effluents that contain organic compounds. The discharge of these compounds without treatment can generate a risk for human health [83]. Therefore, new technologies have been studied for the treatment of water contaminated with these compounds for proper discharge into the environment. Galeano et. al. [83], for example, proposes a method to treat water contaminated with phenolic compounds using an Al/Fe- PILC clay catalyst optimized by statistical tools of experimental design and multi-response surface methodology in CSTR reactor. The catalytic system developed by Galeano et. al. in their work constitutes a good low-cost alternative treatment for the removal of phenolic compounds in contaminated waters.

Sesegma et. al. [39] in his work used Fe/Cu/Al- pillared clays to treat water contaminated with sulfanilamide, obtaining 99-100% pollutant conversions when using these pillared clays as a catalyst. Barrault et. al. [84] were one of the first authors to study the removal of phenol in wastewater using mixed Al/Fe- pillared clays in CWPO. The work reported that approximately 80% of phenol was converted into CO_2 and H_2O within 2 hours of reaction time.

2.4.4.2 Adsorption of pollutants with pillared clays

In the past few years, the study of the modification of clay minerals to increase its adsorption capacity for the removal of pollutants from wastewater has increased [68,69,85]. For example, Ding et. al. [86] prepared Al/Cr- pillared montmorillonite clay materials and tested them for adsorption of benzene. The results obtained show that the benzene adsorption capacity was found to be higher when compared to the starting raw materials. In addition, the results indicated that the material has excellent benzene adsorption performance and that the complete desorption could be achieved in a temperature below the calcination temperature, which indicates that the material could be reused.

Tomul et. al. [87] synthetized Ti-pillared bentonite, Cu, Ag and Fe modified Ti-pillared bentonite and Cu/Ti-bentonite composites using different Ti sources. The adsorption capacity of the Fe/PTi- PILCS sample was observed to be higher when compared to the other samples. The adsorption of bisphenol A by pillared bentonite was found to fit the Langmuir isotherm. It was concluded by Tomul et. al. that the synthesized pillared materials were effective for the adsorption of bisphenol A from aqueous solutions.

MATERIALS AND METHODS

4 MATERIALS AND METHODS

4.1 REACTANTS

The reactants used in this work are given below, separated by the application for which they were used.

Acid activated and pillared clays preparation

- Sulfuric acid (98%). Labkem; Formula: H_2SO_4
- Distilled water
- Acetic acid glacial (99.8%). Fisher Chemical; Formula: $C_4H_2O_2$
- Sodium Acetate (98%). Fisher Chemical; Formula: $C_2H_3NaO_2$
- Iron (III) chloride hexahydrate (99%). Aldrich; Formula: $FeCl_3.6H_2O$
- Cobalt (II) chloride hexahydrate (99%). Fisher Chemical; Formula: $CoCl_2.6H_2O$
- Clays from different deposits of Kazakhstan, namely Akzhar (AKN), Asa (ASN), Karatau (KAN) and Kokshetau (KON)

CWPO runs and analytical techniques

- Paracetamol (98%). Alfa Aesar; Formula: $C_8H_9NO_2$
- Hydrogen peroxide (30% w/v). Fisher Chemical; Formula: H_2O_2
- Titanium (IV) oxysulfate (99.99%). Aldrich; Formula: $TiOSO_4$
- Sulfuric acid (98%). Labkem; Formula: H_2SO_4
- Sodium sulphite anhydrous (98%). Panreac; Formula: Na_2SO_3
- Ultrapure water
- Acid ortho-phosphoric (85%). Riedel-de Haen; Formula: H_3PO_4
- Hydroquinone (99%). Merck KGaA; Formula: $C_6H_6O_2$
- 1, 4-Benzoquinone (99%). Acros Organics; Formula: $C_6H_4O_2$
- Resorcinol (99%). Alfa Aesar; Formula: $C_6H_6O_2$
- 2-Nitrophenol (98%). Aldrich Chemistry; Formula: $C_6H_5NO_3$
- 2-Nitroresorcinol (98%). Alfa Aesar; Formula: $C_6H_5NO_4$
- 4-Nitrocatechol. Fluka (≥ 98%); Formula: $C_6H_5NO_4$

- Pyrocatechol. Fluka (99%); Formula: $C_6H_6O_2$

4.2 PREPARATION OF CLAYS

4.2.1 Acid activated clays

Acid activated clays were prepared by first heating 150 mL of 4 M H_2SO_4 to 80 °C in a three-necked round bottom flask. When the temperature of the system stabilized, 3 g of natural sample in the flask. The resulting suspension was stirred at 80 °C during 3 h. In Figure 9 is shown a picture of the system used in the preparation of the activated clays.

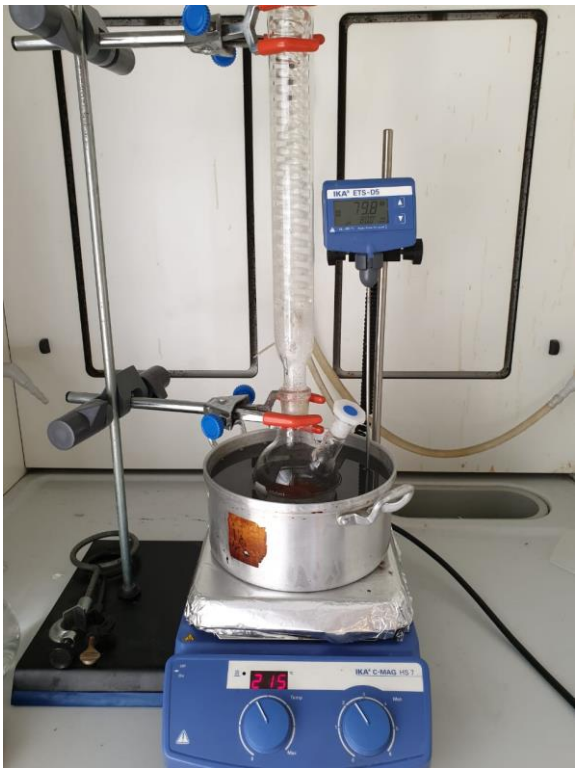

Figure 9. System used for preparing acid activated clays.

After cooling the dispersion, the suspension was filtered and the supernatant discharged. The activated clay was repeatedly washed until the rinsing waters reach a pH close to the natural pH, which is 7. The material was recovered and then dried in an air static oven at 60 °C overnight to obtain the AKA, ASA, KAA and KOA activated clays from AKN, ASN, KAN, and KON, respectively.

4.2.2 Calcined clays

Calcined samples were prepared by thermal treatment. The natural clays AKN, ASN, KAN, and KON were calcined during 5 h at 600 °C in a static air-atmosphere muffle resulting in AKC, ASC, KAC, and KOC, respectively.

4.2.3 Pillared clays

The first step for the preparation of the pillared clays is to the preparation of the pillaring solution, which is shown in Figure 10. The pillaring solution was prepared by mixing appropriate volumes of aqueous 0.5 M Fe^{3+} and 0.25 M Co^{2+} chlorides with a 0.5 M NaOH to obtain a final solution of molar ratio OH/(Fe + Co) = 2:1, with a pH = 2.7. The NaOH was slowly added into the solution containing Fe and Co at room temperature, and later it was left aging during 72 h. Before performing the pillarization, the clays were cleaned with a sodium acetate buffer solution.

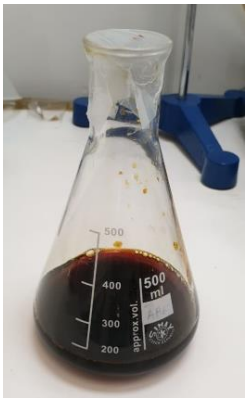

Figure 10. Pillaring solution prepared from 0.5 M Fe^{3+} and 0.25 M Co^{2+} solutions.

For the pillaring process, the aged pillaring solution was added in a 2 wt% suspension for each cleaned clay until reaching a mass ratio of (Fe + Co)/clay = 1:2. The final suspension was stirred at room temperature during 3 h for the intercalation of the metals present in the pillaring solution. After the intercalation step, the suspension was left aging during 72 h and then the material was filtered and washed several times

until the rinsing waters reach the natural pH. In Figure 11**,** it is possible to observe the aspect of the dispersion before and after the 72 h aging.

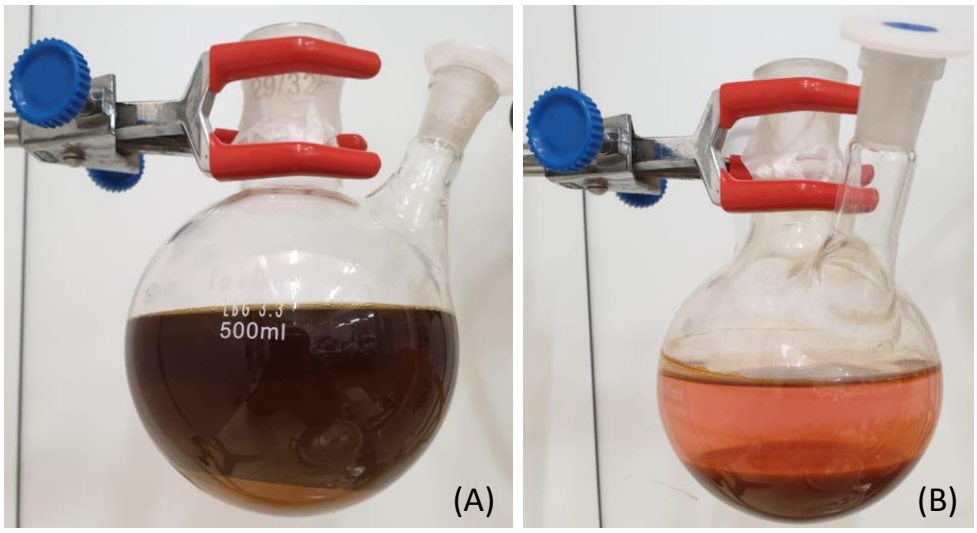

Figure 11. Suspension of clay and pillaring solution A) before and B) after 72 h.

For the last step of the preparation of the pillared clay, the filtered material was dried in an air atmosphere oven at 60 °C overnight and then calcined at 600 °C during 5 h in an air atmosphere muffle. This procedure resulted in the AKP, ASP, KAP and KOP pillared clays from AKN, ASN, KAN, and KON, respectively.

4.3 CHARACTERIZATION TECHNIQUES

4.3.1 Fourier transform infrared spectroscopy (FTIR)

The FTIR spectra of the 16 different samples were recorded on a Perkin Elmer FT-IR spectrophotometer UATR Two infrared spectrophotometer, with a resolution of 4 cm^{-1}. The range of wavenumber used in the analysis was from 450 to 4000 cm^{-1}. All the measurements were done from the solid samples at room temperature.

4.3.2 Surface and pore analyzer

The textural properties of the materials were determined from N_2 adsorption-desorption isotherms at 77 K, obtained in a Quantachrome instrument NOVA TOUCH

LX[4] using long cells with a bulb and an outer diameter of 9 mm. The method of outgassing was done at 120 °C during a period of 16 h, according to the time proposed by IUPAC. The specific surface area (S_{BET}) was calculated by the BET method using the software Quantachrome TouchWin, in the range of p/p_0 0.05 – 0.35.

IUPAC has refined its original classifications of physisorption isotherms and associated hysteresis loops. The new updated classification proposed by IUPAC is shown in Figure 12.

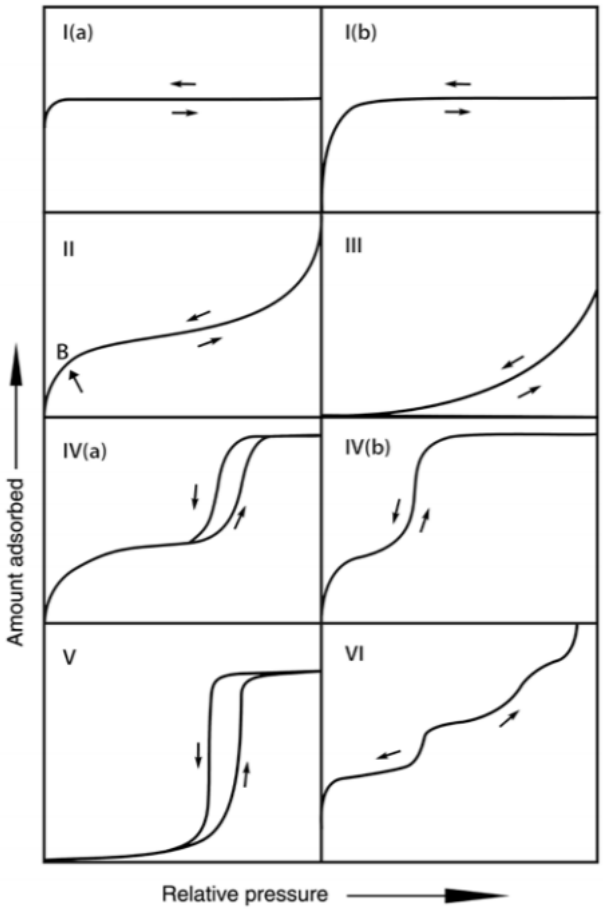

Figure 12. Classification of physisorption isotherms by IUPAC [88].

IUPAC also provides a classification for the hysteresis loop, which is represented in Figure 13.

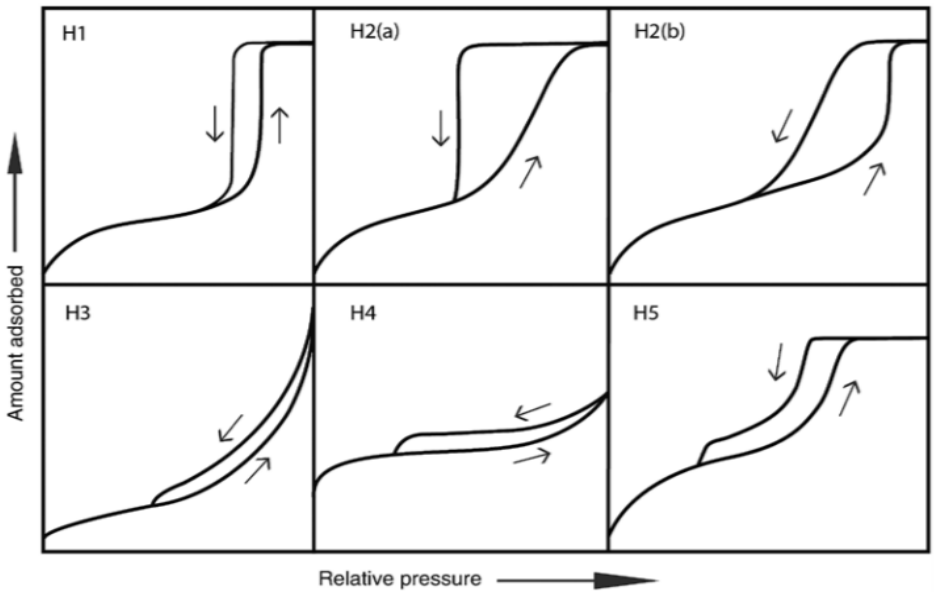

Figure 13. IUPAC classification for hysteresis loop [88].

With these classifications of the isotherms and corresponding hysteresis loop obtained it is possible to characterize the catalysts in terms of the type of material.

4.3.3 X-ray diffraction (XRD)

The measurements of powder X-ray diffraction (XRD) were obtained by depositing the material in the glass sample holder and analyzing on a diffractometer DRON-3.

4.3.4 Acid characterization

One of the tests that can be done for the acid characterization of the clays is the pH of the point of zero charge (pH_{PZC}). For this determination, 0.09 g of clay was added in 6 different erlenmeyers with distinct initial pH values (pH_0). The erlenmeyers were loaded with 15 mL of 0.01 M NaCl and its pH adjusted to different values (2, 4, 6, 8, 10 and 12) by means of 0.02 M NaOH and 0.02 M HCl solutions. The erlenmeyers were placed in an orbital shaker IKA KS 130 Basic and agitated during 24 h at 400 rpm. After the agitation, the suspension was filtered and the pH of the filtrate was measured (pH_F). The pH of the point of zero charge was found in the interception between the curve pH_0 x pH_F and the identity curve.

The second test used in this work for acid characterization is the acidity and basicity determination. In order to determine the acidity and basicity in the different samples, 0.2 g of catalyst was added in 2 different erlenmeyers. One of the erlenmeyers contained 25 mL of a 0.02 M HCl solution for basicity determination, and the other 25 mL of a 0.02 M NaOH solution for acidity determination. The resulting suspensions in the erlenmeyers were placed in an orbital shaker IKA KS 130 Basic and agitated during 48 h at 400 rpm. After the agitation, the suspension of each erlenmeyer was filtered to remove the solid material, and 20 mL was used for determination of the concentration by titration. Knowing the concentration of the resulting solution it is possible to obtain the number of mols that react with the acidic or basic centers of the clay, and then, to calculate the acidity and basicity for each sample. Phenolphthalein was used as an indicator in both titrations.

4.4 CWPO OF PARACETAMOL

4.4.1 Reaction system

Batch oxidation runs were performed under the stoichiometric amount of hydrogen peroxide needed for the complete mineralization of paracetamol, according to the following chemical equation (Eq. (7)):

$$C_8H_9NO_2 + 21H_2O_2 \rightarrow 8CO_2 + HNO_3 + 25H_2O \quad (7)$$

Considering 100 mL of paracetamol solution of 100 mg/L concentration, the amount of hydrogen peroxide necessary to proceed with the experiment was found to be equal to 158 µL of a 30%w/v peroxide solution provided by Sigma Aldrich. The oxidation reactions were carried out in a 250 mL well stirred (600 rpm) round flask reactor, equipped with a condenser and a temperature measurement thermocouple. The reactor was loaded with 100 mL of a 100 ppm paracetamol solution to simulate hospital wastewater effluents, previously acidified until pH 3.5 by means of H_2SO_4. The system was heated by immersion in an oil bath monitored by a temperature controller until 80 °C, which was the temperature used in the oxidation runs. When the temperature stabilized, the stoichiometric amount of hydrogen peroxide was added in the reaction system. After the complete mixing of the reactants, the amount of catalyst necessary to

reach 2.5 g/L was added into the reactor. This moment was then considered as the beginning of the CWPO run (t_0 = 0 min).

The samples for analysis were periodically withdrawn at selected times: 5, 15, 30, 60, 120, 240, 360, 480 and 1440 min. At each time, 3 samples of 1 mL were collected and stored in different eppendorfs, previously prepared according to the analysis that would be done (H_2O_2 concentration, paracetamol concentration, and Total Organic Carbon). Each sample was centrifugated in order to separate the catalyst from the liquid aliquot. After the last sample withdrawal, the catalyst was separated by filtration, the liquid media stored and the catalyst washed with distilled water and dried in an air oven at 60 °C overnight. In Figure 14 it is shown the system used in the CWPO runs.

Figure 14. System used in the CWPO experiments.

4.4.2 Analytical Methods

The quantification of hydrogen peroxide was performed by a colorimetric method, adapting the methodology reported elsewhere [89]. In order to monitor the

concentration of H_2O_2, it was necessary to obtain a calibration curve in the concentration range from 1 to 200 mg/L. For that, 1 mL of different concentration solutions of H_2O_2 was added in a 5 mL volumetric flask with the solution of H_2SO_4 (1 mL/0.5 M) and $TiOSO_4$ (0.1 mL) and then diluted again with distilled water. Then, samples were analyzed by UV–VIS spectrophotometry in a Jasco V-530 at the wavelength of 405 nm to determine its absorbance. The calibration curve obtained with this procedure is represented in Figure 15.

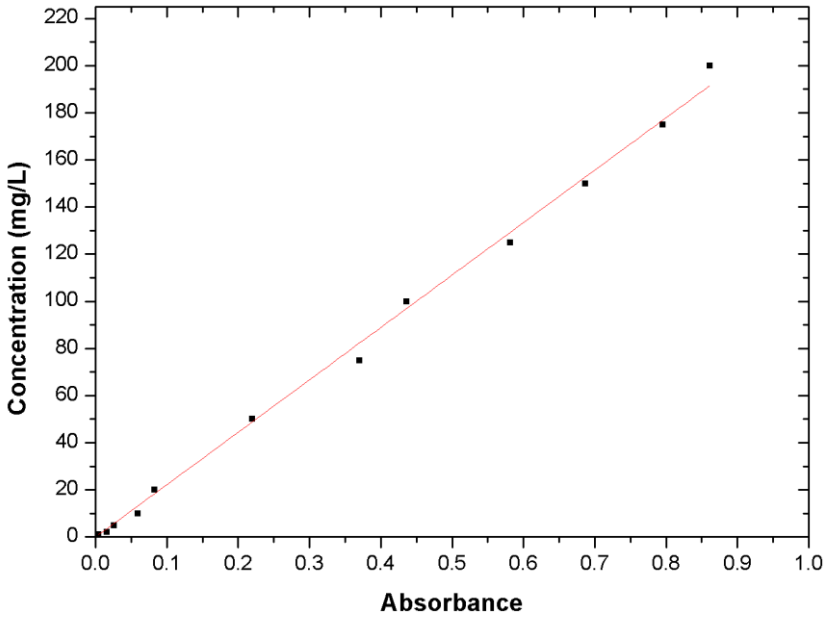

Figure 15. Calibration curve for H_2O_2 determination.

The value of R^2 was found to be 0.997, which shows a good fit for the linear regression.

The determination of hydrogen peroxide concentration of the samples withdrawn from the CWPO reaction media was performed by collecting 1 mL, stored in an eppendorf. Then, the sample was centrifuged, and 0.5 mL of the supernatant was diluted with distilled water in a volumetric flask of 5 mL. From this flask, a sample of 1 mL was withdrawn and added in another volumetric flask of 5 mL containing 1 mL of H_2SO_4 and 0.1 mL of $TiOSO_4$. The absorbance obtained by the UV–VIS analysis of these last samples provided the concentrations of the H_2O_2 along time in the CWPO procedure.

The equipment used for HPLC measurements was a Jasco system equipped with a UV-VIS detector (UV-2075 Plus), a quaternary gradient pump (PU-2089 Plus) for solvent delivery (0.65 mL·min^{-1}) and a RES ELUT 5 µm C18-90Å column (150 mm x 4.6 mm) of VARIAN. With this methodology, it was possible to analyze the model pollutant (paracetamol) and its possible oxidized intermediates, which can be hydroquinone, *p*-benzoquinone, *p*-aminophenol, and *p*-nitrophenol. The wavelength used to measure the peaked absorbance of the compounds was 277 nm. For TOC measurements 1 mL of the samples was diluted in a 20 mL volumetric flask and then analyzed in the equipment SHIMADZU TOC-L.

The quantification of the iron in the remaining solution of CWPO was performed in order to determine the leached iron from the prepared materials to the reaction media. The amount of iron in the samples was determined by atomic absorption, using the equipment SpectrAA Varian equipped with a Varian hollow cathode lamp in a wavelength of 248.3 nm. The first step was to obtain the calibration curve in the range of 0.06-0.2 mg/L. In Figure 16 is given the representation of the calibration curve obtained for the analysis.

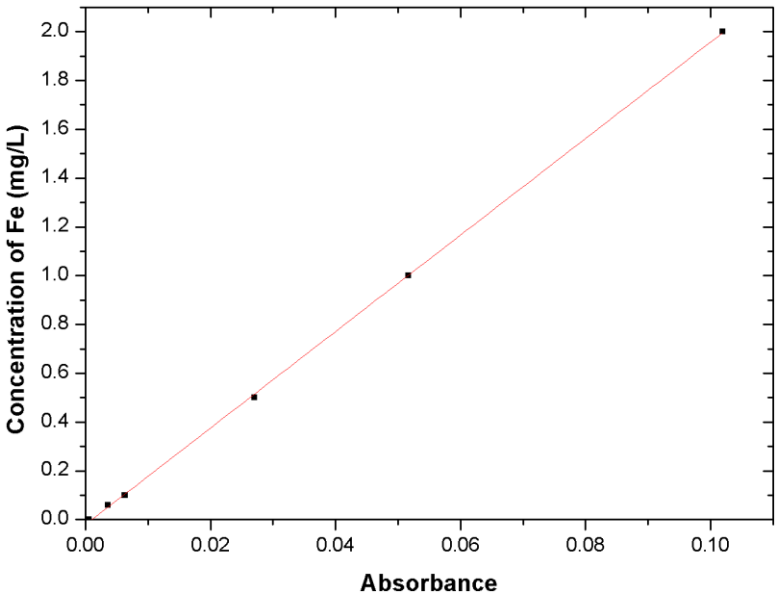

Figure 16. Calibration curve for iron leached measurements.

The value of R^2 was found to be 0.999, which shows a good fit for the linear regression. The wastes of the CWPO runs were filtered in a 45 µm membrane and the supernatant was stored in a vial and then analyzed in the equipment, in order to obtain

its absorbance and consequently the iron concentration. Another parameter relevant to the analysis of this result is the percentage of iron leached from the clay structure. For the pillared clays, it is possible to find such a parameter since the amount of iron used to synthesize the pillared clays is known. Using stoichiometry calculations it was found that the maximum concentration of iron possible to leach into solution during the CWPO runs is 818.23 mg/L for the runs that used pillared clays as a catalyst. With this value and the results of iron leaching obtained in the CWPO runs with pillared clays it was possible to calculate the percentage of iron leached from the clay structure.

4.4.3 Adsorption

For the adsorption tests, 25 mL of the same paracetamol solution used in the CWPO runs (100 mg/L) runs was added in an erlenmeyer loaded with 0.625 g of catalyst (2.5 g/L of catalyst concentration). The erlenmeyer was placed in an orbital shaker IKA KS 130 Basic and agitated during 24 h at 400 rpm. After the agitation, the suspension was filtered and the filtrate was analyzed in the HPLC for analysis of the paracetamol concentration. The percentage of paracetamol adsorbed was calculated by the difference between the initial and the final concentration.

RESULTS AND DISCUSSION

5 RESULTS AND DISCUSSION

5.1 CHARACTERIZATION OF MATERIALS

The prepared materials were tested by Fourier Transformed Infra-Red (FTIR), adsorption isotherms of N_2, X-ray diffractions (XRD) and acidity/basicity determination.

5.1.1 Fourier Transform Infra-Red spectroscopy (FTIR)

The FTIR spectra obtained by analysis of the different prepared clays are depicted in Figure 17.

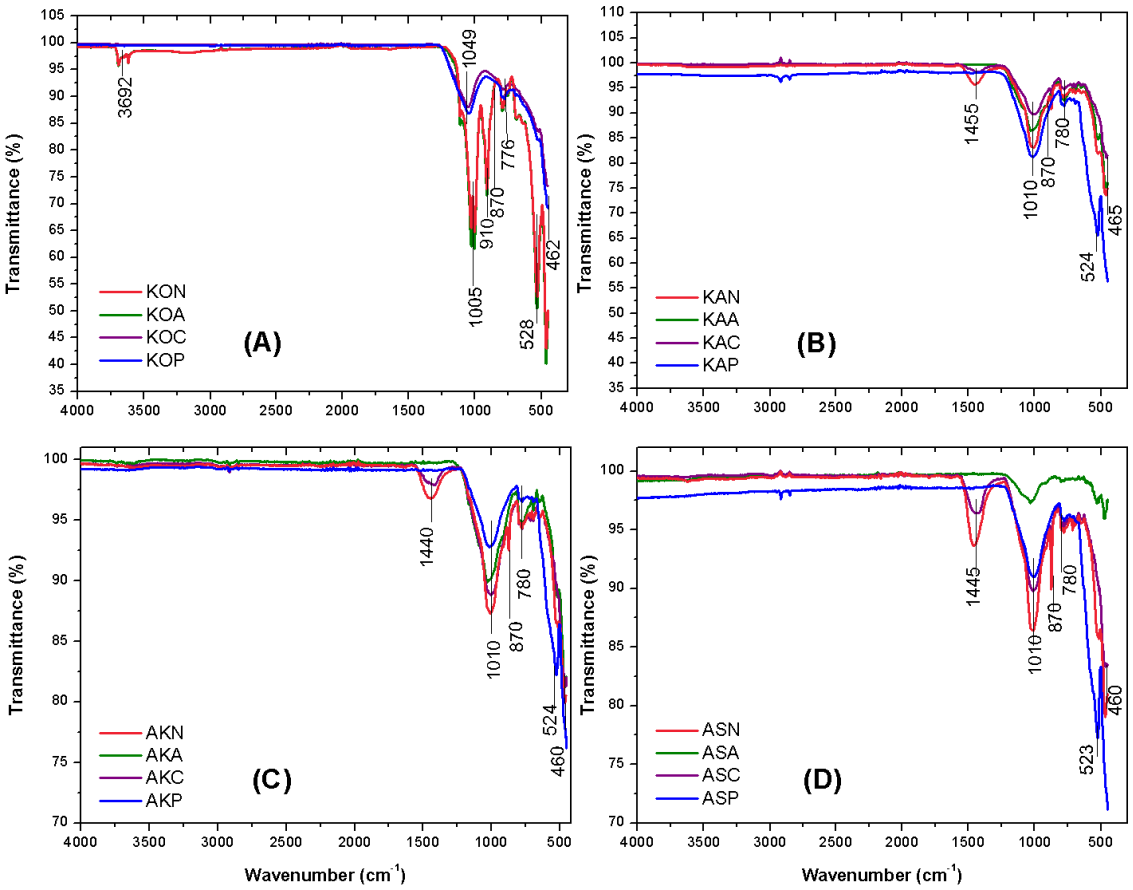

Figure 17. FTIR spectra of the A) Kokshetau clays, B) Karatau clays, C) Akzhar clays and D) Asa clays.

In the Kokshetau spectra given in Figure 17(A), it is possible to observe a band appearing at 3,692 cm^{-1} for the natural clay. This band is due to the –OH stretching vibration for water adsorbed at the interlayer, reason why this signal is absent in the samples subjected to a calcination treatment [74]. This band has no signal in other clays because the amount of adsorbed water in its interlayer is not significant. Observing the spectra of Akzhar, Asa, and Karatau clays, it is possible to realize that the natural clays and the calcined clays have a band in the range of 1,440 – 1,455 cm^{-1}. This band is due to the presence of calcite in the materials, and its disappearance is a consequence of the exchange between calcium and the pillaring metals, indicating the success of the pillarization [90]. That band was found to be absent in the FTIR spectra of the pillared clays and of the activated clays, explained by the fact that the acid treatment and the pillaring process causes a structural modification. This band has no signal for the Kokshetau sample because the amount of calcite in its structure is not significant.

The band in the range of 1,005 to 1,010 cm^{-1} is present in the spectra of all samples and represents the stretching vibrations of the Si–O bond group [91]. For the Kokshetau activated and natural samples, there is a signal at 910 cm^{-1}, assigned to Al-OH-Al bonds [77]. The band at 870 cm^{-1} for natural samples can be ascribed to the Al-Mg-OH bending vibrations. The reduction of its intensity in the spectra of the pillared samples occurs by the fact that structural treatments cause the fracture of these bonds [74]. The absence of transmittance in this band in the spectra of the pillared samples also could mean that the cation Mg^{2+} was exchanged in the pillaring procedure by the pillaring cations used. In the range of wavenumber from 776 to 780 cm^{-1}, there is a signal of transmittance attributed to the presence of quartz impurity [92].

The band present in the range of 523 to 528 cm^{-1} is associated with the bending vibrations of the group Si–O–Mg [93]. The last band, which is present in the range of 460 to 465 cm^{-1}, represents important information deserving special attention. This band is related to the presence of bending vibrations of Si–O–Fe bonds, which is present in all of the samples, since the natural clays also contain an amount of these bonds in its structure [94,95]. The important part is that in the Asa, Akzhar, Karatau and Kokshetau pillared samples, the signal of the transmittance in this band is present, which suggests the successful incorporation of Fe by the pillaring process in the structure of the clay.

5.1.2 Surface and pore analysis

The adsorption isotherms of N_2 at 77 K on prepared samples are depicted in Figure 18.

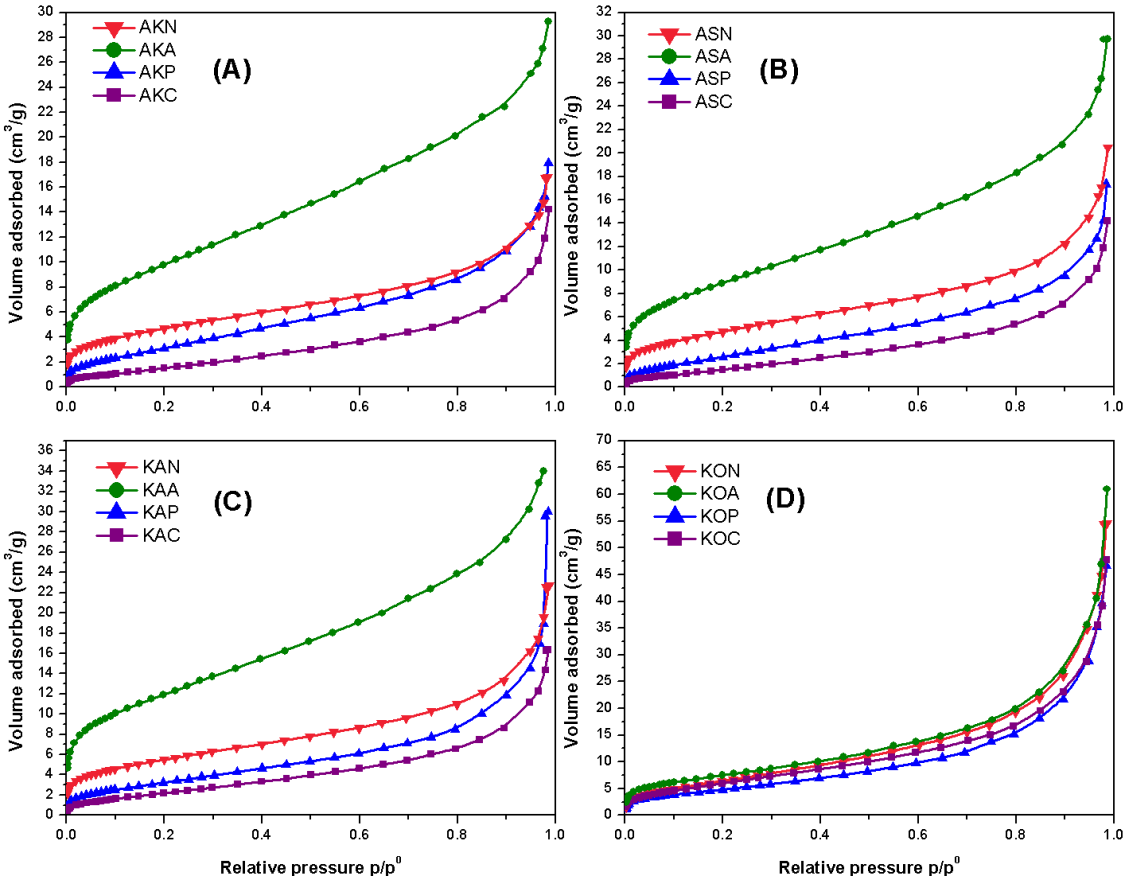

Figure 18. Adsorption isotherms of N_2 at 77 K of the A) Akzhar clays, B) Asa clays, C) Karatau clays and D) Kokshetau clays.

As can be observed, the acid activated materials show the highest adsorption capacity when compared to the natural, calcined and pillared clays. The higher adsorption for the activated sample is less visible for Kokshetau clay, and this occurs because the acid treatment was not able to significantly increase the surface area of this material. Besides that, the same tendency can be observed in Akzhar, Asa, and Karatau samples, with higher adsorption being obtained in the activated sample followed by the natural, the pillared and the calcined samples. According to the IUPAC classification, it is possible to conclude that the physisorption isotherms obtained in this work fits in Type II. This classification is attributed to nonporous or macroporous adsorbents, for

which the shape of the isotherm is a result of unrestricted monolayer-multilayer adsorption up to high p/p^0. For these materials, the beginning of the middle almost linear section (around p/p^0 = 0.02 in this work) usually corresponds to the completion of monolayer coverage. After this point, a more gradual curvature is an indication of a significant amount of overlap of monolayer coverage and the onset of multilayer adsorption [88].

The results of S_{BET} obtained from the adsorption isotherms are shown in Table 3.

Table 3. S_{BET} from the materials.

Material	S_{BET} (m^2/g)	Material	S_{BET} (m^2/g)
AKN	17	KAN	20
AKA	35	KAA	43
AKC	7	KAC	9
AKP	13	KAP	13
ASN	17	KON	26
ASA	32	KOA	28
ASC	8	KOC	24
ASP	11	KOP	19

The values in Table 3 confirm that the materials with highest BET surface area are the acid activated clays, which represents a good result since the main goal of this kind of treatment is to increase the surface area of the material. The pillared clays presented a lower surface area than that of the natural clays. This effect occurred by the fact that the calcination treatment done as the last step of the pillaring procedure may have caused the collapse of the pillars. This supposition is valid taking into consideration some works reporting that above 400 °C the pillars collapse in some samples, and this can be the case in this work. Another explanation for the result obtained could be the blockage of the pores of the material with the particles of iron and cobalt, as a consequence of the high concentration of these metals in the pillaring solution.

The adsorption-desorption isotherms of N_2 at 77 K is represented in Figure 19 for the materials with the highest adsorbed N_2 volumes in each series (acid activated clays).

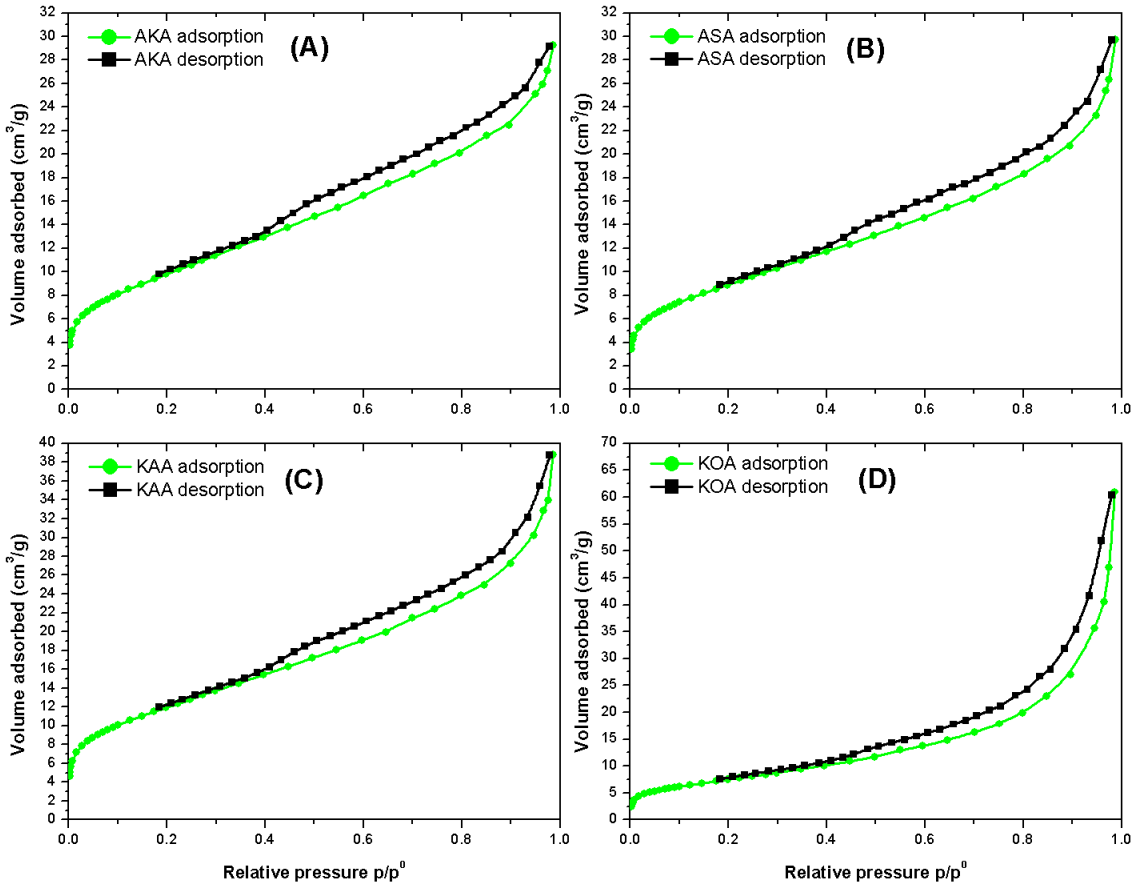

Figure 19. Adsorption-desorption curves for the materials with highest S_{BET}.

Comparing the hysteresis loops of the materials in Figure 19 with the IUPAC classification for hysteresis loops, it is possible to conclude that the materials have a H3 type. There are two features that allow the identification of this hysteresis loop: the adsorption branch for this loop resembles a Type II isotherm and the lower limit of desorption branch is normally located at the cavitation-induced p/p^0. This type is typically found in non-rigid aggregates of plate-like particles, as for examples certain clays [88]. Other materials (natural, calcined and pillared clays) show similar hysteresis loops, as can be observed in the attachments for the calcined samples (Figure 27), natural samples (Figure 28) and pillared samples (Figure 29).

5.1.2 X-Ray Diffraction (XRD)

For this analysis, it was chosen a set of materials that could give more interesting results, such as Karatau and Kokshetau that has the pillared samples with the higher surface area. In order to determine the composition of the crystalline phases of the

Karatau and Kokshetau samples, these were subjected to X-ray diffractometric analysis. For the interpretation of the results, the software HighScore Demo was used, from PANanalytical. Figure 20 gathers the XRD diffractograms of the analyzed samples.

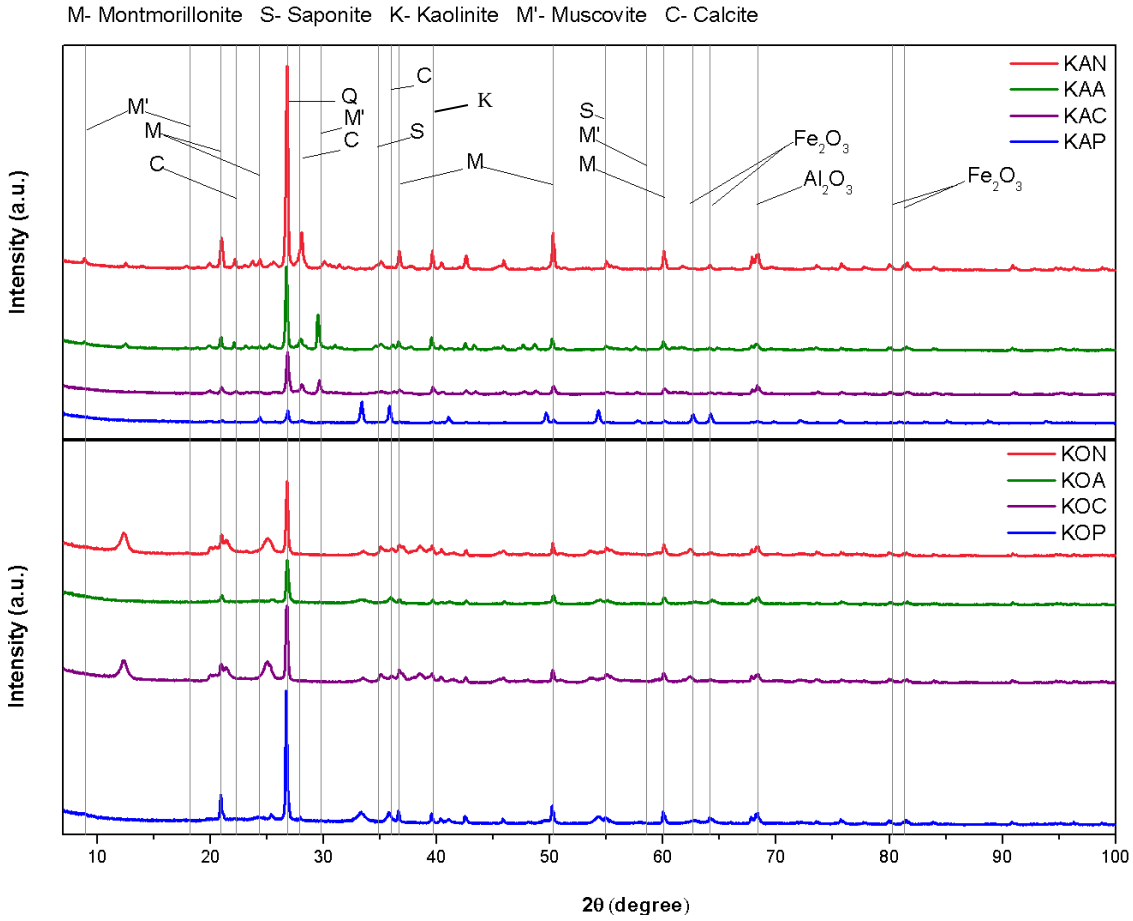

Figure 20. XRD diffractograms of the A) Karatau samples and B) Kokshetau samples.

Observing the XRD patterns obtained, it is possible to realize that both clays present the typical reflection of montmorillonite [96]. As the samples were provided from natural deposits, it was expected that its crystal composition was formed not only by one clay mineral but by multiple phases. Thus, in KAN it is also possible to find traces of saponite [97], kaolinite [98] and muscovite [99], confirming the composition of this clay obtained in another study [100]. In KON, in addition to the already mentioned montmorillonite, there is also the correspondence for the presence of kaolinite [97]. All the samples present a peak at 26.7° related to the presence of quartz (SiO_2 impurities), as also identified in other studies [93,101]. The analysis of the diffractograms also allowed the identification of calcite for the Karatau sample and the absence of calcite for Kokshetau

samples, which corroborates with FTIR results. Even knowing that the clays present not only montmorillonite in its crystal composition, the intensities of the peaks in the positions referred to this mineral are higher than the intensities assigned to the other phases, suggesting that the clays are majority composed by montmorillonite. Therefore, both clays can be classified as bentonite, which is the denomination given to the class of clays composed by a mixture of different clay minerals, with a majority composition of montmorillonite [24].

It is possible to observe that the signal for SiO_2 [102] and metal oxides such as aluminum oxide [103] and iron oxide [103] decreased in the diffractograms of the Karatau and Kokshetau samples after the acid treatment. This can be explained by the fact that the acid treatment washed the impurities of SiO_2 from the clay structure, also leaching a small amount of iron metals. For the calcined sample KAC, the behavior observed is a little different to that observed for KAA, since the signal of iron oxides is maintained. Therefore, the signal for SiO_2 decreased more in the diffractogram of KAC than in that of KAA and the signal for metal oxides, as iron oxide and aliminum oxide, was about the same as found in the diffractogram of KON. For the pillared sample KAP it is possible to observe that the signal for the SiO_2 impurities decreased, and that the signal for the iron oxide increased significantly, putting in evidence the incorporation of iron in the material. In fact, the signal attributed to iron oxide in this sample was higher than in the others.

In the diffractogram of KOC, the signals attributed to iron and alumina oxides were the same as those obtained in the diffractogram of KON, and the signal attributed to SiO_2 had a small decrease. Finally, in the diffractogram of KOP, the signal for iron oxide was significantly higher than in that observed for the natural sample KON, also confirming the successful incorporation of iron in the clay structure. Besides all the differences between the signals in both diffractograms of the Karatau and Kokshetau samples, it is interesting to observe that the signal for montmorillonite, kaolinite, saponite, and muscovite wasn't significantly changed in the different samples. This suggests that the structure of the clay is stable, although passing through some structural changes the main structure remained [104].

5.1.4 Acid characterization

The origin of the electrical charge in the structure of the clays is of two kinds: a permanent charge resulting from the isomorphic substitution of Al^{3+} or Si^{4+} in the mineral structure and a variable (pH dependent) charge resulting from proton adsorption/desorption reaction on the surface [105]. Depending on the pH, the surface of the clay can bear negative, or positive or no charge. The pH where the net total particle is zero is called the point of zero charge (pH_{PZC}). This parameter is one of the most important parameters used to describe variable-charge surfaces [106]. Another test that can be done to corroborate with the pH_{PZC} results is the determination of acidity and basicity. The acidity and basicity results can also be used to observe the effect of the treatments used in the preparation of the activated and pillared samples.

Following the procedure described in the methodology for the calculation of the pH_{PZC}, the result was obtained by the interception of the experimental curves with the identity. Figure 21 shows the measurements of pH for the determination of the pH_{PZC}.

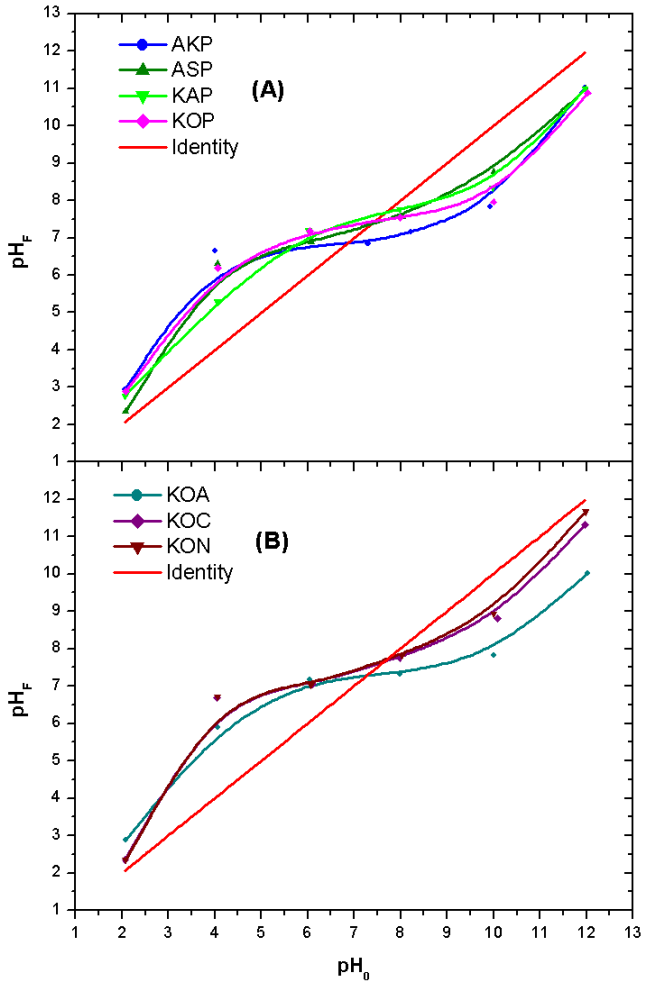

Figure 21. pH_{pzc} curves for A) Pillared samples B) KOA, KOC and KON samples.

Using the graphic exposed it is possible to find the pH_{PZC}. For the acidity and basicity determination, the procedure described in the methodology was followed and the results for the acid characterization are summarized in Table 4**.**

Table 4. Results for the acid characterization.

Samples	Acidity (µmol/g)	Basicity (µmol/g)	pH_{PZC}
AKP	812	538	7.15
ASP	475	372	7.55
KAP	687	627	7.42
KOP	950	652	7.37
KOA	987	614	7.24
KOC	337	270	7.67
KON	350	245	7.77

The results obtained for acidity and basicity show that this feature is weak for the samples. As can be observed, all pillared clays have a similar result for the pH_{PZC}, with a difference in the decimal case. An interesting comparison can be done between the samples KOA, KOC, KON, and KOP. According to specific studies of pH_{PZC} of pillared clays is expected that the result for the pillared clay is lower than the result obtained with the natural sample [107]. For this work, even than small, it is possible to observe that there is a difference between the pH_{PZC} of the KON and the pH_{PZC} of the KOP, showing that structural modification has occurred in the clay. Not only the KOP but also the KOA present a different result for pH_{PZC}, which suggests that structural modifications also occurred with the acid treatment.

The measurement of the acidity and basicity showed that most of the samples are acids. It is possible to observe also that the acidity is higher for the samples that have a lower value for the pH_{PZC}, which confirms the results obtained by the analysis. Comparing again the samples KOA, KOC, KON and KOP it is possible to conclude that the acid and pillaring treatments caused an increase in the acidity and in the difference between the acidity and basicity in comparison with the natural sample. Between the pillared samples, the KOP is the one that shows the highest acidity and basicity.

The majority of the previous works regarding the use of clay-based materials in catalytic procedures do not perform an acid quantitative characterization [108,109]. Some works even treat about the acid and basic sites of Lewis but using a qualitative methodology that does not allow the quantification of the acidity and basicity, limiting to qualify the samples [87,107,110]. Different from the other works done so far, in this work

the methodology used for the acid characterization allowed the quantification of the acidity and basicity from the samples.

5.2 EXPERIMENTAL REACTIONS

A set of prepared materials were chosen to be used as a catalyst in the CWPO of paracetamol. In order to evaluate the efficiency of each material, the concentration of paracetamol, H_2O_2, and TOC were followed along time. Adsorption tests were performed with all the samples, in order to evaluate if its removal is significant.

5.2.1 Catalytic Wet Peroxide Oxidation (CWPO)

As in this work, there are 16 different materials, some materials were selected to be used in the CWPO of paracetamol. In this sense, all pillared clays were chosen to be tested as a catalyst for the CWPO of paracetamol, since they have iron in its structure as a consequence of pillaring process, that is expected to work as the active phase. The pillared sample that presented the better result for the CWPO had its respective activated, calcined and natural samples analyzed for the catalysis. Figure 22 shows the concentration of H_2O_2 and paracetamol as a function of the time of reaction.

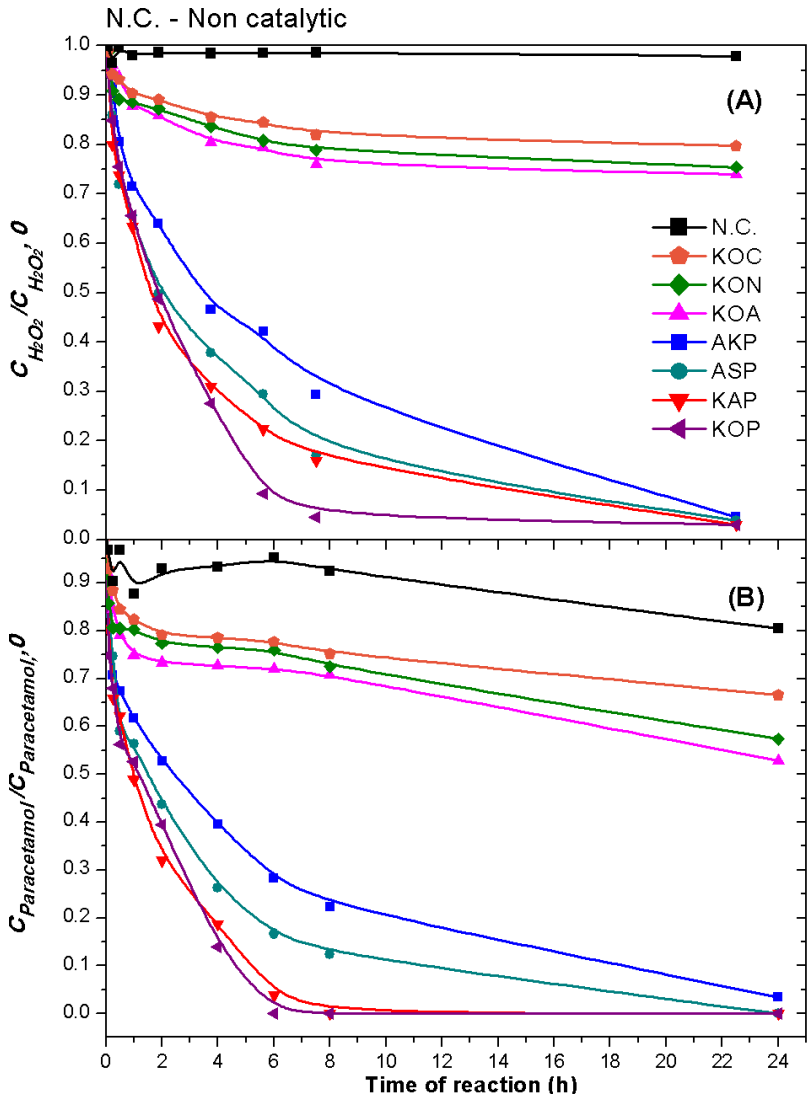

Figure 22. (A) Normalized concentration of H_2O_2 along time. (B) Normalized concentration of paracetamol along time, under the operational conditions: $C_{Paracetamol}$ = 100 mg/L, $C_{H_2O_2}$ = 472.4 mg/L, C_{cat} = 2.5 g/L.

Analyzing the concentration profile of paracetamol in Figure 22B, it is interesting to observe that all the pillared materials showed catalytic activity, enabling the decomposition of H_2O_2 and allowing to reach a conversion of hydrogen peroxide higher than 90% after 24 h. In addition, it is possible to conclude that the material with the best activity is the KOP, with the full conversion of paracetamol between 240 and 360 min of reaction. In addition, KOA, KOC, and KON had its performance in CWPO analyzed for comparison purposes. Figure 22A supports the hypothesis that KOP had the best activity, once that presented the faster conversion of H_2O_2 compared with the other materials. The best activity for the KOP can be explained by the fact that between the pillared materials, its surface area, acidity, and basicity are the highest.

The result obtained for the CWPO of the activated, calcined and natural samples for Kokshetau also exhibits interesting results. Both 3 materials presented a low conversion of paracetamol after 24 h, and the low conversion of H_2O_2 for these materials supports this result. The worst material is the calcined, with a conversion of paracetamol of 33.4% after 24 h, which can be explained by the fact that the calcination decreased the surface are of the material. The slight best result obtained with the KOA when compared with the KON has meaning since the surface area of KOA is higher than in KON

To the best of my knowledge, there is no other work that uses pillared clays in the CWPO of paracetamol. However, there are works regarding the degradation of paracetamol by heterogeneous Fenton-like process [111] and photo-Fenton [112]. Using a heterogeneous Fenton-like process, the same initial concentration used in this work and $[catalyst]_0$ = 6 g/L Velichkova et. al. [111] obtained full conversion of pollutant within 5 h of reaction, while in this work more than 90% of the pollutant was degraded within 4 h of reaction using the best catalyst, KOP. Alalm et. al. [112] used the photo-Fenton process for the removal of paracetamol, with the same initial concentration of pollutant used in this work and $[H_2O_2]_0$ = 1,500 mg/L, and reached the full conversion of paracetamol within 60 minutes of reaction. Although the good result, the amount of hydrogen peroxide used by Alalm et. al. was 217.8% higher than the stoichiometric concentration necessary to degrade the pollutant, besides that, in their work it was used irradiation as a source of energy for the Fenton.

The results also show the influence of 2 parameters of the catalysts for the CWPO: the surface area and the presence of iron. The surface area of KOA is higher than the KOP, even so, the KOP presented a higher activity for the CWPO. This can be explained by the fact that in the KOP sample there is also much more iron than in KOA structure, and this makes the KOP more active than KOA.

The analysis of TOC was performed with the samples withdrawn from the reaction media at different times. The results are represented in Figure 23.

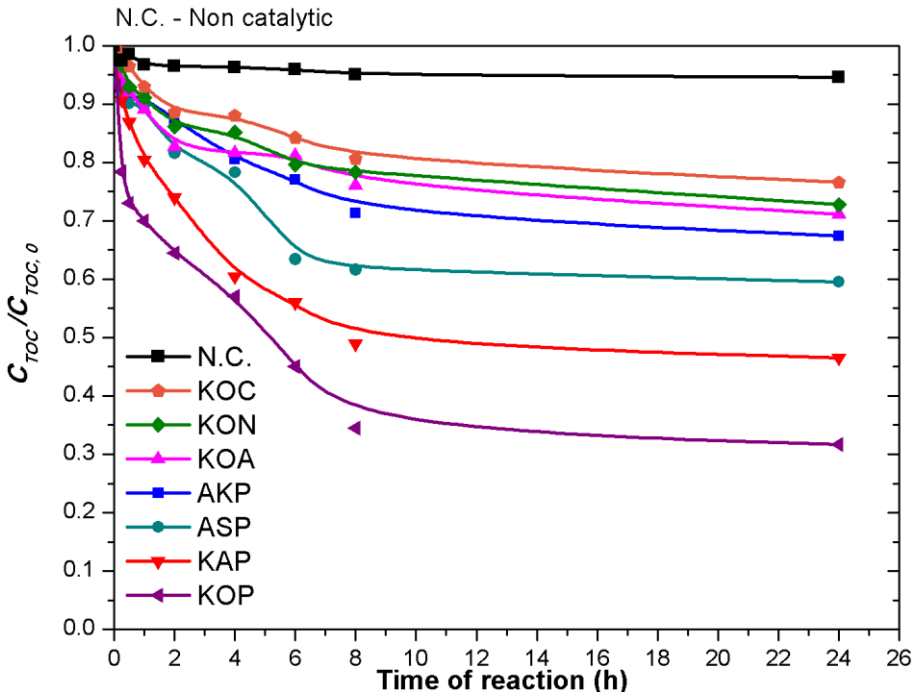

Figure 23. Normalized concentration of TOC along time under the operational conditions: $C_{Paracetamol}$ = 100 mg/L, $C_{H_2O_2}$ = 472.4 mg/L, C_{cat} = 2.5 g/L.

As can be observed the pillared materials presented the higher conversions of TOC, which agrees with the results obtained so far for the paracetamol and H_2O_2 conversion. In fact, for all the three analysis the ascending order for the conversions is KOC, KON, KOA, AKP, ASP, KAP and KOP, which gives more representativeness for the result, once that the tendency was obeyed for the correlated analysis. The pillared materials presented an appreciable conversion, in this case, the best material was the KOP, with a conversion that reached incredible 68.3% of mineralization. Comparing the results obtained by the KOA, KOC, KON, and KOP the result obtained before it repeats, with the pillared material having the best behavior, followed by the activated, natural and calcined material. This can be explained by the fact that the pillared material has more iron than the others, and the activated has more surface area in comparison with the natural and calcined ones.

There is in the literature previous works that analyze the TOC in the CWPO of paracetamol, such as the work done by Trovó et. al. [113] and Velichkova et. al. [111], with photo-Fenton and heterogeneous Fenton reactions, respectively. With an initial concentration of paracetamol of 50 mg/L, at 25 °C, and operating conditions of $[H_2O_2]_0$ = 120 mg/L and $[catalyst]_0$ = 0.05 mM, Trovó reached 79% of mirealization using as catalyst $FeSO_4.7H_2O$. Even though the work is done by Trovó et. al. present higher

mineralization than in this work, the author used irradiation as a source of energy for the Fenton. In the work done by Velichkova et. al. the higher mineralization achieved with the best material was 43%, which is 25.3% less than the mineralization obtained in this work using the best catalyst, KOP.

The determination of iron leached was made at the end of each CWPO reaction, and the results obtained are presented in Table 5.

Table 5. Fe leached at the end of the CWPO experiments.

Samples	Concentration of leached iron (mg/L)	Leaching of iron (wt%)
AKP	0.0971	0.0119
ASP	0.0159	0.0019
KAP	0.0179	0.0022
KOP	0.0892	0.0109
KOA	0.0101	N. A.
KOC	0.1742	N. A.
KON	0.1762	N. A.
Non catalytic	0.0001	N. A.

***N. A. = Not Applied**

The results obtained for all the materials are very satisfactory, once that they are all below the limit concentration of 2 mg/L of iron in water, established by the law. The information about the percentage of iron leached it also suggests that the pillared clays are stable catalysts, once that for all these samples less than 0.1% of the iron present in the structure was leached. Comparing the results obtained for pillared materials it is possible to observe that the material with the lower stability is AKP, once that it is the material with high iron leaching. The more stable material, between the pillared is the ASP because in this case, it is the material with the lower iron leaching.

An interesting comparison can be done between KOA, KOC, KON and KOP materials. The results suggested that the pillaring procedure increased the stability of the material since the iron leaching obtained for the pillared material is lower than the obtained for the natural and calcined ones. In addition, the result for the activated

material showed the lower result between the 4 materials, and this can be explained by the fact that the activated treatment removed an amount of iron from the structure of the clay, and then the leaching of the iron is lower when compared with the natural sample. As the most active material in this work is the pillared kokshetau, is interesting to compare its iron leaching with other results for the same analysis obtained by other works regarding the use of pillared clays in CWPO. In the work done by Carriazo et. al. [53], pillared clays with Fe and Cu were used in the removal of phenol from the water, and the results of iron leaching vary from 0.05 until 0.6 mg/L for the different materials, which either values are higher than the value obtained in this work.

The TOC, paracetamol, H_2O_2 conversion, and leached iron are represented in Figure 24.

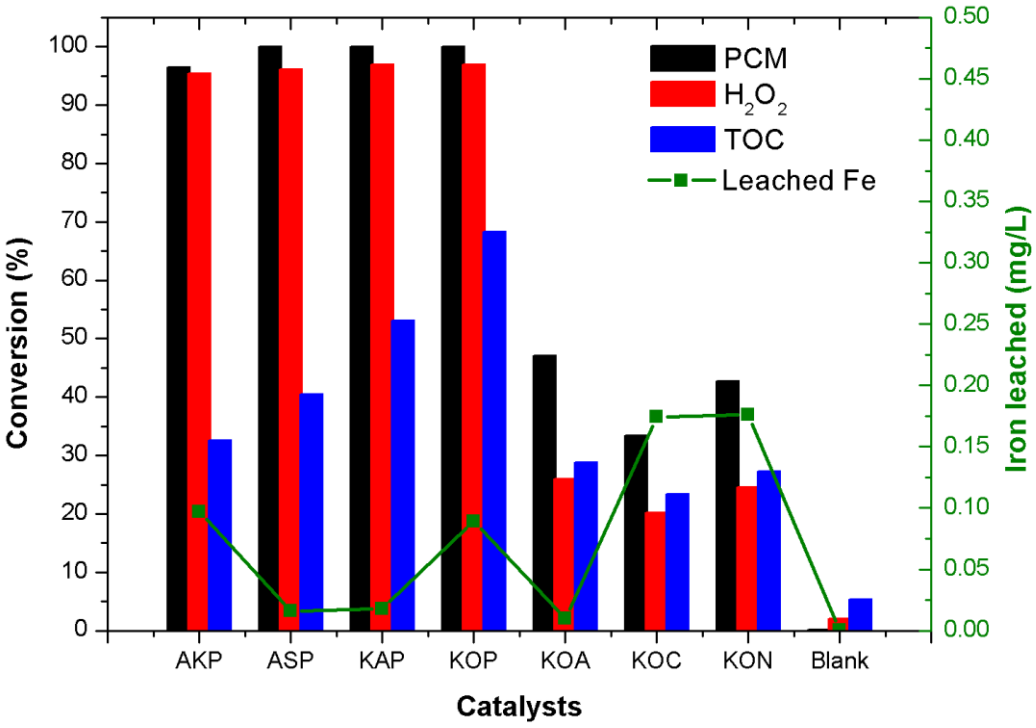

Figure 24. Reached conversion and concentration of leached iron in aqueous media solutions after 24 h of reaction time.

Analyzing the results in the graphic, it is possible to observe that for our material the iron leaching was lower for the materials with higher conversions. This suggests that the pillaring procedure increased the stability of the material, which represents a good result since the pillared materials removed paracetamol more efficiently. Other authors

as Carriazo et. al. [53] have reported this behavior in pillared clays. In fact, Carriazo et. al. showed also that increasing the amount of iron as pillaring metal, the leaching of this metal decreases.

5.2.2 Adsorption

In order to confirm if the removal of the pollutant is occurring by means of the oxidation process or if the pollutant is only being adsorbed on the materials, is interesting to perform adsorption tests. The result obtained for paracetamol removal after 24 h in the adsorption tests compared with the oxidation process after 8 and 24 his exposed in Figure 25.

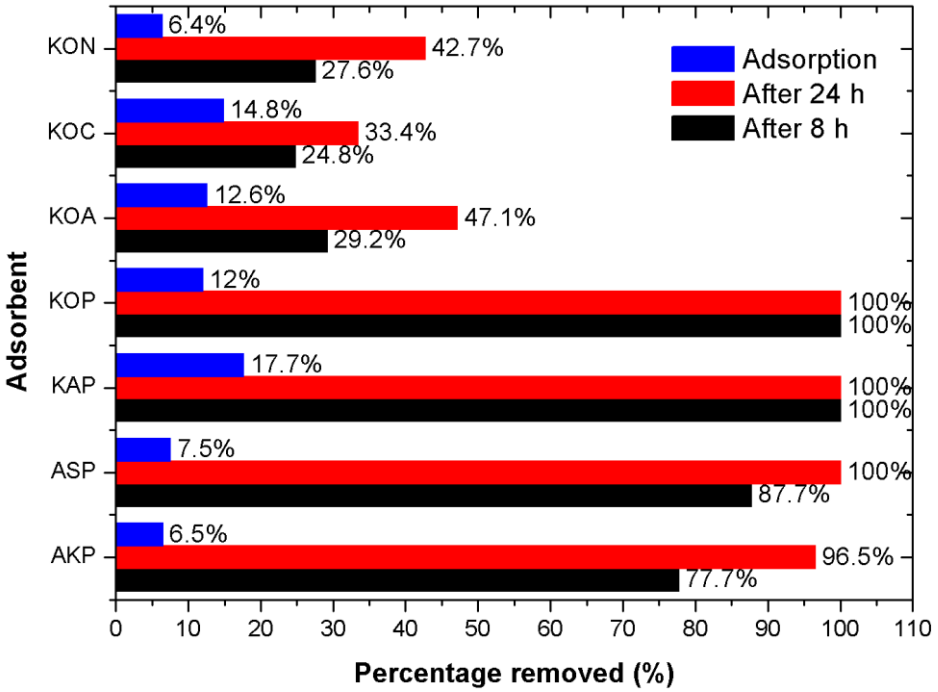

Figure 25. Comparison between removal of paracetamol with adsorption after 24 h and CWPO after 8 h and 24 h.

The results for adsorption of paracetamol using the synthesized materials showed that after 24 h, the percentage of pollutant adsorbed varied from 4 until 18%. On the other hand, after 8 h paracetamol had already been completely converted for the CWPO procedure using KAP and KOP materials as a catalyst. Furthermore, the pollutant was more than 95% converted after 24 h of CWPO for all the pillared samples.

Even for the samples not pillared, the conversion of paracetamol in CWPO after 24 h showed to be higher than its removal by adsorption. Thus, it is possible to discard the possibility of the paracetamol be being mostly adsorbed and not oxidized. Due to its simplicity, the adsorption tests for paracetamol were done for all the samples used in this work. The result obtained for all the samples is shown in Figure 26.

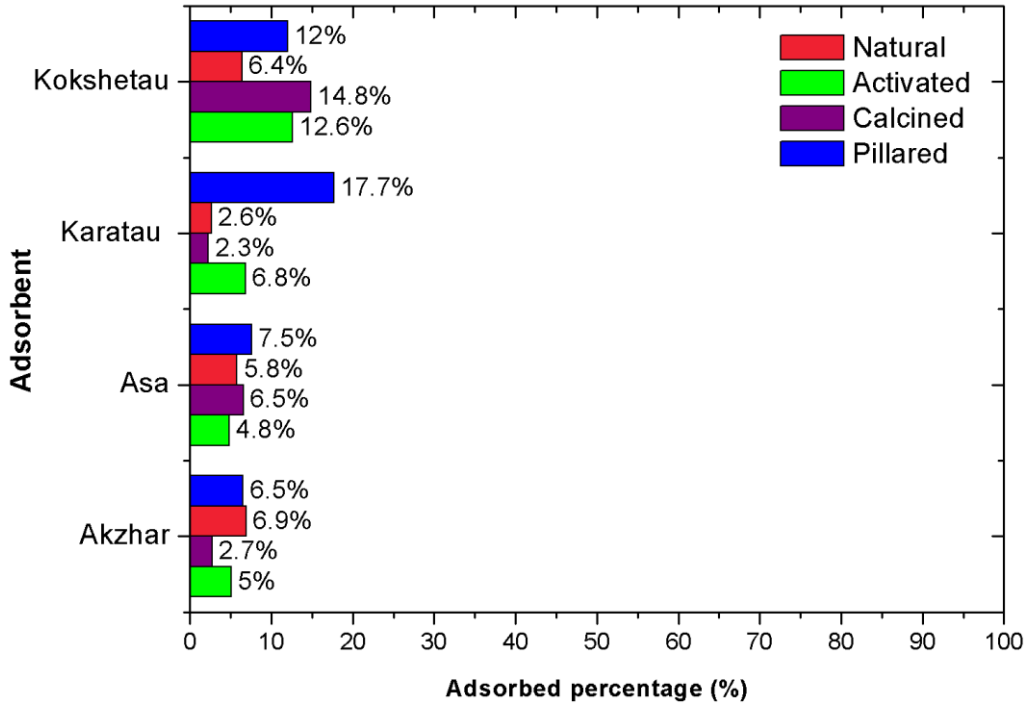

Figure 26. Adsorption of paracetamol.

As the graphic shows, for adsorption tests, the results varied from 4 until 18% of pollutant adsorbed. The adsorption results for the model pollutant were not significant for all of the samples, and the result obtained for the pillared samples prove that the removal of paracetamol is occurring by an oxidation process in the CWPO runs. To the best of my knowledge, there is no other work regarding CWPO that has made an adsorption test to ensure that the pollutant is being removed by means of oxidation and not adsorption, so this is another differential in this work.

CONCLUSIONS AND FUTURE WORK

6 CONCLUSIONS AND FUTURE RESEARCH

6.1 CONCLUSIONS

The treatment of wastewater containing paracetamol is viable by CWPO with the clay-based catalyst prepared from natural clays by acid activation or pillarization. The CWPO runs done with pillared clays as catalyst leads to more than 90% removal of the pollutant within 24 h of reaction at the operating conditions of 80 °C, C_{cat} = 2.5 g/L and $C_{Paracetamol}$ = 100 mg/L. The clay catalysts prepared by activation with H_2SO_4 or pillarization with Co and Fe show catalytic activity in the process when compared with the non-catalytic wet péroxide oxidation of paracetamol at the same operating conditions. In addition, pure adsorption runs showed a maximum contribution in the removal of the pollutant between 4-18%, clarifying that the removal of the pollutant by CWPO is mainly due to the oxidation, instead of adsorption.

All prepared materials tested in CWPO allow to remove from 33.4% until 100% after 24 h with the operating conditions of 80 °C, C_{cat} = 2.5 g/L and $C_{Paracetamol}$ = 100 mg/L. The highest catalytic activity was found for Kokshetau pillared clay, that was prepared from the clay obtained in Kokshetau deposits. This was ascribed to some important features of the material, such as the higher amount of iron in its structure, the higher acidity, and the higher surface area when compared to the other materials prepared in this work. The CWPO with this material leads to the complete conversion of pollutant between 240 and 360 minutes of reaction, and mineralization of 68.3%.

6.2 FUTURE RESEARCH

Clay-based materials have been synthesized from 4 different natural clays obtained from deposits of Kazakhstan and later prepared clays have been characterized and used as a catalyst in the treatment of wastewater effluents containing a model pharmaceutical component by CWPO. All the pillared clays presented catalytic activity in the CWPO of paracetamol, which was the chosen model pollutant in this work.

It would be interesting for future works evaluate the effect of the conditions during the pillarization of the clays in order to increase the performance of the resultant materials, once that many parameters are involved in the procedure. The pillaring solution, which defines the metals incorporated in the clay structure, could be prepared

keeping the iron, that is known as the main active phase in CWPO process, and using another metals such as copper and aluminum, which are more used in the pillaring procedure and have shown good results in other works [53,63,114–116]. An important parameter that could be also changed is the calcination, which is responsible for the formation of the pillars in the clay structure. This procedure could be more soft, using a maximum temperature of 400 °C, once that for higher temperatures occurs fractures in the pillars [117]. Another interesting analysis would be the use of the catalysts for the CWPO of real effluents, containing not only one pollutant but a set of pollutants. This would allow the evaluation of the catalysts in a different matrix, closer to reality.

An alternative work that could be done with the clays is the preparation of a magnetic material to be used as a catalyst in the removal of organic pollutants. An example of material is the magnetic nanoparticle coprecipitated with clay mineral, typically known as MNP/CM. It could be prepared the Fe_3O_4/CM by coprecipitation using the KAA, which is the clay with a higher surface area. The material prepared in this work would certainly be good for the catalysis because it would have a good surface area and a high amount of iron. Beyond the good features for a catalyst in CWPO, the material would be magnetic, and magnetic materials have been very explored lately.

REFERENCES

7 REFERENCES

1. Gutiérrez, F., Parise, M., De Waele, J. & Jourde, H. A review on natural and human-induced geohazards and impacts in karst. *Earth-Science Rev.* **138**, 61–88 (2014).
2. McNamara, K. E. The global casino: an introduction to environmental issues (Fifth Edition). *Aust. Plan.* **51**, 370–370 (2014).
3. Djalante, R. Review Article: Adaptive governance and resilience: the role of multi-stakeholder platforms in disaster risk reduction. *Nat. Hazards Earth Syst. Sci.* **12**, 2923–2942 (2012).
4. Klamerth, N., Malato, S., Maldonado, M. I., Agüera, A. & Fernández-Alba, A. R. Application of Photo-Fenton as a tertiary treatment of emerging contaminants in municipal wastewater. *Environ. Sci. Technol.* **44**, 1792–1798 (2010).
5. Postigo, C., López de Alda, M. J. & Barceló, D. Drugs of abuse and their metabolites in the Ebro River basin: Occurrence in sewage and surface water, sewage treatment plants removal efficiency, and collective drug usage estimation. *Environ. Int.* **36**, 75–84 (2010).
6. Charuaud, L., Jarde, E., Jaffrezic, A., Thomas, M.-F. & Le Bot, B. Veterinary pharmaceutical residues from natural water to tap water: Sales, occurrence and fate. *J. Hazard. Mater.* **361**, 169–186 (2019).
7. Villota, N., Lomas, J. M. & Camarero, L. M. Kinetic modelling of water-color changes in a photo-Fenton system applied to oxidate paracetamol. *J. Photochem. Photobiol. A Chem.* **356**, 573–579 (2018).
8. Silva, C. P., Jaria, G., Otero, M., Esteves, V. I. & Calisto, V. Waste-based alternative adsorbents for the remediation of pharmaceutical contaminated waters: Has a step forward already been taken? *Bioresour. Technol.* **250**, 888–901 (2018).
9. Munoz, M., de Pedro, Z. M., Casas, J. A. & Rodriguez, J. J. Preparation of magnetite-based catalysts and their application in heterogeneous Fenton oxidation – A review. *Appl. Catal. B Environ.* **176**–**177**, 249–265 (2015).
10. Homem, V. & Santos, L. Degradation and removal methods of antibiotics from aqueous matrices – A review. *J. Environ. Manage.* **92**, 2304–2347 (2011).
11. Slamani, S., Abdelmalek, F., Ghezzar, M. R. & Addou, A. Initiation of Fenton process by plasma gliding arc discharge for the degradation of paracetamol in

water. *J. Photochem. Photobiol. A Chem.* **359**, 1–10 (2018).

12. Akhi, Y., Irani, M. & Olya, M. E. Simultaneous degradation of phenol and paracetamol using carbon/MWCNT/Fe_3O_4 composite nanofibers during photo-like-Fenton process. *J. Taiwan Inst. Chem. Eng.* **63**, 327–335 (2016).
13. Abdel-Wahab, A.-M., Al-Shirbini, A.-S., Mohamed, O. & Nasr, O. Photocatalytic degradation of paracetamol over magnetic flower-like TiO_2 /Fe_2O_3 core-shell nanostructures. *J. Photochem. Photobiol. A Chem.* **347**, 186–198 (2017).
14. Augusto, T. de M., Poliane, C., Daniel, L. S., Tatiana, M. L., Cristina, O., Castro, C. Iron ore tailings as catalysts for oxidation of the drug paracetamol and dyes by heterogeneous Fenton. *J. Environ. Chem. Eng.* **6**, 6545–6553 (2018).
15. Do, Q. C., Kim, D.G., Ko, S.O. Catalytic activity enhancement of a Fe_3O_4@SiO_2 Yolk-shell structure for oxidative degradation of acetaminophen by decoration with copper. *J. Clean. Prod.* **172**, 1243–1253 (2018).
16. Glaze, W. H., Kang, J. W. & Chapin, D. H. The chemistry of water treatment processes involving ozone, hydrogen peroxide and ultraviolet radiation. *Ozone Sci. Eng.* **9**, 335–352 (1987).
17. Audino, F., Conte, L., Scheone, A., Graells, M., Alfano, O. A kinetic study for the fenton and photo-fenton paracetamol degradation in a pilot plant reactor. in *Computer Aided Chemical Engineering* 301–306 (Elsevier Masson SAS, 2017). doi:10.1016/B978-0-444-63965-3.50052-0
18. Diaz de Tuesta, J. L., Quintanilla, A., Casas, J. A. & Rodriguez, J. J. Kinetic modeling of wet peroxide oxidation with a carbon black catalyst. *Appl. Catal. B Environ.* **209**, 701–710 (2017).
19. Tehrani-Bagha, A. R. & Balchi, T. Catalytic wet peroxide oxidation, Chapter 12. in *Advanced Oxidation Processes for Waste Water Treatment* 375–402 (Elsevier, 2018). doi:10.1016/B978-0-12-810499-6.00012-7
20. Datta, S. & Torrente-Murciano, L. Nanostructured faceted ceria as oxidation catalyst. *Curr. Opin. Chem. Eng.* **20**, 99–106 (2018).
21. Sheng, Y., Kraft, M. & Xu, R. Emerging applications of nanocatalysts synthesized by flame aerosol processes. *Curr. Opin. Chem. Eng.* **20**, 39–49 (2018).
22. Aznárez, A., Delaigle, R., Eloy, P., Gaigneaux, E. M., Gil, A. Catalysts based on pillared clays for the oxidation of chlorobenzene. *Catal. Today* **246**, 15–27

(2015).

23. Baloyi, J., Ntho, T. & Moma, J. Synthesis and application of pillared clay heterogeneous catalysts for wastewater treatment: a review. *RSC Adv.* **8**, 5197–5211 (2018).
24. Widjaya, R. R., Juwono, A. L. & Rinaldi, N. Bentonite modification with pillarization method using metal stannum. in *AIP Conference Proceedings* 1–7 (2017). doi:10.1063/1.5011867
25. Hong, Y. W., Yuan, D. X., Lin, Q. M. & Yang, T. L. Accumulation and biodegradation of phenanthrene and fluoranthene by the algae enriched from a mangrove aquatic ecosystem. *Mar. Pollut. Bull.* **56**, 1400–1405 (2008).
26. Madikizela, L. M., Tavengwa, N. T. & Chimuka, L. Status of pharmaceuticals in African water bodies: Occurrence, removal and analytical methods. *J. Environ. Manage.* **193**, 211–220 (2017).
27. He, Z., Cheng, X., Kyzas, G. Z. & Fu, J. Pharmaceuticals pollution of aquaculture and its management in China. *J. Mol. Liq.* **223**, 781–789 (2016).
28. Fent, K., Weston, A. & Caminada, D. Ecotoxicology of human pharmaceuticals. *Aquat. Toxicol.* **76**, 122–159 (2006).
29. C. G. Daughton, T. A. T. Pharmaceuticals and personal care products in the environment: agents of subtle change? *Environ. Health Perspect.* **107**, 907–938 (1999).
30. Ferroudj, N., Nzimoto, J., Anne, D., Talbot, D., Brito, E., Dupuis, V., Bée, A, Medjaram, M. S., Abramson, S. Maghemite nanoparticles and maghemite/silica nanocomposite microspheres as magnetic Fenton catalysts for the removal of water pollutants. *Appl. Catal. B Environ.* **136**–**137**, 9–18 (2013).
31. Fekadu, S., Alemayehu, E., Dewil, R. & Van der Bruggen, B. Pharmaceuticals in freshwater aquatic environments: A comparison of the African and European challenge. *Sci. Total Environ.* **654**, 324–337 (2019).
32. Busca, G., Berardinelli, S., Resini, C. & Arrighi, L. Technologies for the removal of phenol from fluid streams: A short review of recent developments. *J. Hazard. Mater.* **160**, 265–288 (2008).
33. Ribeiro, A. R., Nunes, O. C., Pereira, M. F. R. & Silva, A. M. T. An overview on the advanced oxidation processes applied for the treatment of water pollutants defined in the recently launched Directive 2013/39/EU. *Environ. Int.* **75**, 33–51 (2015).

34. Diniz, M. S., Maurício, R., Petrovic, M., Maria, A., Amaral, L., Peres, I., Damiá, B., Santana, F. Assessing the estrogenic potency in a Portuguese wastewater treatment plant using an integrated approach. *J. Environ. Sci.* **22**, 1613–1622 (2010).
35. Bethi, B., Sonawane, S. H., Bhanvase, B. A. & Gumfekar, S. P. Nanomaterials-based advanced oxidation processes for wastewater treatment: A review. *Chem. Eng. Process. Process Intensif.* **109**, 178–189 (2016).
36. Liotta, L. F., Gruttadauria, M., Di Carlo, G., Perrini, G. & Librando, V. Heterogeneous catalytic degradation of phenolic substrates: Catalysts activity. *J. Hazard. Mater.* **162**, 588–606 (2009).
37. Pignatello, J. J., Oliveros, E. & MacKay, A. Advanced oxidation processes for organic contaminant destruction based on the fenton reaction and related chemistry. *Crit. Rev. Environ. Sci. Technol.* **36**, 1–84 (2006).
38. Frost, C., Shenker, A., Gandhi, M., Pursley, J., Barrett, Y. C., Wang, J., Zhand, D., Byon, W.Boyd, R., LaCreta, F. Evaluation of the effect of naproxen on the pharmacokinetics and pharmacodynamics of apixaban. *Br. J. Clin. Pharmacol.* **78**, 877–885 (2014).
39. Khankhasaeva, S. T., Dashinamzhilova, E. T. & Dambueva, D. V. Oxidative degradation of sulfanilamide catalyzed by Fe/Cu/Al-pillared clays. *Appl. Clay Sci.* **146**, 92–99 (2017).
40. Jones, C. W. Environmental applications of hydrogen peroxide , Chapter 5. in *Applications of hydrogen peroxide and derivatives* (Royal Society of Chemistry, 1999). doi:10.1039/9781847550132
41. Kaloidas, V., Koufopanos, C. A., Gangas, N. H. & Papayannakos, N. G. Scale-up studies for the preparation of pillared layered clays at 1 kg per batch level. *Microporous Mater.* **5**, 97–106 (1995).
42. Martin-Martinez, M., García, J., Silva, A., Faria, J., Gomes, H. T. Exploring the activity of chemical-activated carbons synthesized from peach stones as metal-free catalysts for wet peroxide oxidation. *Catal. Today* **313**, 20–25 (2018).
43. Escapa, C., Coimbra, R. N., Paniagua, S., García, A. I. & Otero, M. Paracetamol and salicylic acid removal from contaminated water by microalgae. *J. Environ. Manage.* **203**, 799–806 (2017).
44. Mackay, D., Shiu, W. Y., Ma, K. C., Lee, S. C. Phenolic compounds, Chapter 14. in *Handbook of physical properties of organic chemicals.* 2779–3023 (2006).

45. Tomul, F. Effect of ultrasound on the structural and textural properties of copper-impregnated cerium-modified zirconium-pillared bentonite. *Appl. Surf. Sci.* **258**, 1836–1848 (2011).
46. Witko, M., Hermann, K. & Tokarz, R. Adsorption and reactions at the (010) V_2O_5 surface: cluster model studies. *Catal. Today* **50**, 553–565 (1999).
47. Song, M., Wang, Y., Guo, Y., Wang, L., Zhan, W., Lu, G. Catalytic wet oxidation of aniline over Ru catalysts supported on a modified TiO_2. *Chinese J. Catal.* **38**, 1155–1165 (2017).
48. Rey, A., Faraldos, M., Casas, J. A., Bahamonde, A., Rodríguez, A. A. Catalytic wet peroxide oxidation of phenol over Fe/AC catalysts: Influence of iron precursor and activated carbon surface. *Appl. Catal. B Environ.* **86**, 69–77 (2009).
49. Zhao, Q., Mao, Q., Zhou, Y., Wei, J., Liu, X., Yang, J., Luo, L., Zhang, J., Chen, H., Tang, L. Metal-free carbon materials-catalyzed sulfate radical-based advanced oxidation processes: A review on heterogeneous catalysts and applications. *Chemosphere* **189**, 224–238 (2017).
50. Gomes, H. T., Miranda, S. M., Sampaio, M. J., Silva, A. M. T. & Faria, J. L. Activated carbons treated with sulphuric acid: Catalysts for catalytic wet peroxide oxidation. *Catal. Today* **151**, 153–158 (2010).
51. Rey, A., Faraldos, M., Bahamonde, A., Casas, J., Zazo, J., Rodríguez, J. Role of the activated carbon surface on catalytic wet peroxide oxidation. *Ind. Eng. Chem. Res.* **47**, 8166–8174 (2008).
52. Ribeiro, R. S., Silva, A. M. T., Figueiredo, J. L., Faria, J. L. & Gomes, H. T. Removal of 2-nitrophenol by catalytic wet peroxide oxidation using carbon materials with different morphological and chemical properties. *Appl. Catal. B Environ.* **140**–**141**, 356–362 (2013).
53. Carriazo, J. G., Guelou, E., Barrault, J., Tatibouët, J. M. & Moreno, S. Catalytic wet peroxide oxidation of phenol over Al–Cu or Al–Fe modified clays. *Appl. Clay Sci.* **22**, 303–308 (2003).
54. Carretero, M. I. Clay minerals and their beneficial effects upon human health. *Appl. Clay Sci.* **21**, 155–163 (2002).
55. F. Bergaya, G. L. General introduction, Cahpter 1. in *Clays, Clay Minerals, and Clay Science* (2006). doi:10.1016/B978-0-08-098258-8.00001-8Get
56. Cecilia, J. A., García-Sancho, C., Vilarrasa-García, E., Jiménez-Jiménez, J. &

Rodriguez-Castellón, E. Synthesis, characterization, uses and applications of porous clays heterostructures: A review. *Chem. Rec.* **18**, 1085–1104 (2018).

57. Shi, H., Lan, T. & Pinnavaia, T. J. Interfacial Effects on the reinforcement properties of polymer−organoclay nanocomposites. *Chem. Mater.* **8**, 1584–1587 (1996).
58. Bian, Z. & Kawi, S. Preparation, characterization and catalytic application of phyllosilicate: A review. *Catal. Today* (2018). doi:S0920586118309921
59. Cool, P. & Vansant, E. F. The principle of pillaring, Chapter 2. in *Pillared Clays : Preparation , Characterization and Applications* 266–268 (1998).
60. Gil, A., Korili, S. A., Trujillano, R. & Vicente, M. A. A review on characterization of pillared clays by specific techniques. *Appl. Clay Sci.* **53**, 97–105 (2011).
61. Galeano, L.-A., Vicente, M. Á. & Gil, A. Catalytic degradation of organic pollutants in squeous dtreams by mixed Al/M-pillared clays (M = Fe, Cu, Mn). *Catal. Rev.* **56**, 239–287 (2014).
62. Li, J., Hu, M., Zuo, S. & Wang, X. Catalytic combustion of volatile organic compounds on pillared interlayered clay (PILC)-based catalysts. *Curr. Opin. Chem. Eng.* **20**, 93–98 (2018).
63. Khalaf, H., Bouras, O. & Perrichon, V. Synthesis and characterization of Al-pillared and cationic surfactant modified Al-pillared Algerian bentonite. *Microporous Mater.* **8**, 141–150 (1997).
64. Suzuki, K., Mori, T. & Hirate-cho, N. Preparation of alumina - pillared montmorillonite with desired pillar population. *Pergamon Press* **23**, 1711–1718 (1988).
65. Salles, F., Douillard, J., Deyonel, R., Bildstein, O., Jullien, M., Beurroies, I., Van Damme, H. Hydration sequence of swelling clays: Evolutions of specific surface area and hydration energy. *J. Colloid Interface Sci.* **333**, 510–522 (2009).
66. Bijang, C., Wahab, A. W., Ahmad, A. & Taba, P. Study of Calcination Temperatures of Pillared Bentonite to the Performance of Cyanide Biosensor and its Application to Determine Cyanide in Cassava. *J. New Mater. Electrochem. Syst.* **18**, 005–008 (2015).
67. Hernando, M. J., Pesquera, C., Blanco, C., Benito, I. & González, F. Differences in structural, textural, and catalytic properties of montmorillonite pillared with ($GaAl_{12}$) and ($AlAl_{12}$) polyoxycations. *Chem. Mater.* **8**, 76–82 (1996).

68. Wang, K., Yan, X. & Komarneni, S. CO_2 Adsorption by several types of pillared montmorillonite clays. *Appl. Petrochemical Res.* **8**, 173–177 (2018).

69. Zhao, D., Wang, G., Yang, Y., Guo, X., Wang, Q., Ren, J. Preparation and characterization of hydroxy-FeAl pillared clays. *Clays Clay Miner.* **41**, 317–327 (1993).

70. Moreno, S., Kou, R. S., Molina, R. & Poncelet, G. Al-, Al,Zr-, and Zr-Pillared montmorillonites and saponites: Preparation, characterization, and catalytic activity in heptane hydroconversion. *J. Catal.* **182**, 174–185 (1999).

71. Best, J. P., Wehrs, J., Polyakov, M., Morstein, M. & Michler, J. High temperature fracture toughness of ceramic coatings evaluated using micro-pillar splitting. *Scr. Mater.* **162**, 190–194 (2019).

72. Rhodes, C. N., Franks, M., Parkes, G. M. B. & Brown, D. R. The effect of acid treatment on the activity of clay supports for ZnCl2 alkylation catalysts. *J. Chem. Soc. Chem. Commun.* 804–807 (1991). doi:10.1039/c39910000804

73. Yu, W., Wang, P., Zhou, C., Zhao, C., Tong, D., Zhang, H., Ji, S., Wang, H. Acid-activated and WO_x -loaded montmorillonite catalysts and their catalytic behaviors in glycerol dehydration. *Chinese J. Catal.* **38**, 1087–1100 (2017).

74. Li, T., Zhao, L., Zheng, Z., Zhang, M., Sun, Y., Tian, Q., Zhang, S. Design and preparation acid-activated montmorillonite sustained-release drug delivery system for dexibuprofen in vitro and in vivo evaluations. *Appl. Clay Sci.* **163**, 178–185 (2018).

75. Sabu, K. ., Sukumar, R., Rekha, R. & Lalithambika, M. A comparative study on H_2SO_4, HNO_3 and $HClO_4$ treated metakaolinite of a natural kaolinite as Friedel–Crafts alkylation catalyst. *Catal. Today* **49**, 321–326 (1999).

76. Zhao, H., Zhou, C., Wu, L., Lou, J., Li, N., Yang, H., Tong, D. S., Yu, W. H. Catalytic dehydration of glycerol to acrolein over sulfuric acid-activated montmorillonite catalysts. *Appl. Clay Sci.* **74**, 154–162 (2013).

77. Zatta, L., Ramos, L. P. & Wypych, F. Acid-activated montmorillonites as heterogeneous catalysts for the esterification of lauric acid acid with methanol. *Appl. Clay Sci.* **80**–**81**, 236–244 (2013).

78. Xavier, K. C. M., Santos, M., Oliveira, M., Carvalho, M., Osajima, J., Silva Filho, E. Effects of acid treatment on the clay palygorskite: XRD, surface area, morphological and chemical composition. *Mater. Res.* **17**, 3–08 (2014).

79. Bieseki, L., Treichel, H., Araujo, A. S. & Pergher, S. B. C. Porous materials

obtained by acid treatment processing followed by pillaring of montmorillonite clays. *Appl. Clay Sci.* **85**, 46–52 (2013).

80. Vuković, Z. Abu-Rabi, A., Novakovic, T., Jovanovic, D. The influence of acid treatment on the nanostructure and textural properties of bentonite clays. *Mater. Sci. Forum* **494**, 339–344 (2005).
81. Mache, J. R., Signing, P., Mbey, J. A., Fagel, N., Mineralogical and physico-chemical characteristics of Cameroonian smectitic clays after treatment with weakly sulfuric acid. *Clay Miner.* **50**, 649–661 (2015).
82. Panda, A. K., Mishra, B. G., Mishra, D. K. & Singh, R. K. Effect of sulphuric acid treatment on the physico-chemical characteristics of kaolin clay. *Colloids Surfaces A Physicochem. Eng. Asp.* **363**, 98–104 (2010).
83. Ramírez, J. H., Galeano, L. A., Pinchao, G., Bedoya, R. A. & Hidalgo, A. Optimized CWPO phenol oxidation in CSTR reactor catalyzed by Al/Fe-PILC from concentrated precursors at circumneutral pH. *J. Environ. Chem. Eng.* **6**, 2429–2441 (2018).
84. Barrault, J., Abdellaoui, M., Bouchoule, A., Majesté, A., Louloudi, I., Gangas, N. H. Catalytic wet peroxide oxidation over mixed pillared (Al–Cu) clays. *Appl. Catal. B Environ.* **130**, 749–754 (2000).
85. Tireli, A. A., Guimarães, I. do R., Terra, J. C. de S., da Silva, R. R. & Guerreiro, M. C. Fenton-like processes and adsorption using iron oxide-pillared clay with magnetic properties for organic compound mitigation. *Environ. Sci. Pollut. Res.* **22**, 870–881 (2015).
86. Liu, J., Dong, M., Zuo, S. & Yu, Y. Solvothermal preparation of TiO_2/montmorillonite and photocatalytic activity. *Appl. Clay Sci.* **43**, 156–159 (2009).
87. Tomul, F., Turgut Basoglu, F. & Canbay, H. Determination of adsorptive and catalytic properties of copper, silver and iron contain titanium-pillared bentonite for the removal bisphenol A from aqueous solution. *Appl. Surf. Sci.* **360**, 579–593 (2016).
88. Thommes, M., Kaneko, K., Neimark ,A., Oliver, J., Rouquerol, J., Sing, K. Physisorption of gases, with special reference to the evaluation of surface area and pore size distribution (IUPAC Technical Report). *Pure Appl. Chem.* **87**, 1051–1069 (2015).
89. Masso, C. M., Gomes, H. T., Pietrobelli, J. M. T. & Tuesta, J. L. D. De.

Valorization of compost in the production of carbon-based materials for the treatment of contaminated wastewater Valorization of compost in the production of carbon-based materials for the treatment of contaminated wastewater. *Mestrado IPB* (2018).

90. Bruckman, V. J., Wriessnig, K. Improved soil carbonate determination by FT-IR and X-ray analysis. *Environ. Chem. Lett.* **11**, 65–70 (2013).
91. Jain, S. & Datta, M. Montmorillonite-alginate microspheres as a delivery vehicle for oral extended release of Venlafaxine hydrochloride. *J. Drug Deliv. Sci. Technol.* **33**, 149–156 (2016).
92. Komadel, P. Acid activated clays: Materials in continuous demand. *Appl. Clay Sci.* **131**, 84–99 (2016).
93. Yuan, P., Tao, Q., Fan, M., Liu, Z., Zhu, J., He, H., Chen, T. A combined study by XRD, FTIR, TG and HRTEM on the structure of delaminated Fe-intercalated/pillared clay. *J. Colloid Interface Sci.* **324**, 142–149 (2008).
94. Eren, E. & Afsin, B. An investigation of Cu(II) adsorption by raw and acid-activated bentonite: A combined potentiometric, thermodynamic, XRD, IR, DTA study. *J. Hazard. Mater.* **151**, 682–691 (2008).
95. Wang, S., Dong, Y., He, M., Chen, L. & Yu, X. Characterization of GMZ bentonite and its application in the adsorption of Pb(II) from aqueous solutions. *Appl. Clay Sci.* **43**, 164–171 (2009).
96. Trigueiro, P., Rodrigues, F., Rigaud, B., Balme, S., Janot, J., Fonseca, M., Osajima, J., Walter, P. When anthraquinone dyes meet pillared montmorillonite: Stability or fading upon exposure to light? *Dye. Pigment.* **159**, 384–394 (2018).
97. Sprynskyy, M., Sokol, H., Rafísnka, K., Buszewski, B. Preparation of AgNPs/saponite nanocomposites without reduction agents and study of its antibacterial activity. *Colloids Surfaces B Biointerfaces* **180**, 457–465 (2019).
98. Zhu, B. L., Qi, C., Zhang, Y., Bisson, T., Xu, Z., Fan, Y., Sun, Z. Synthesis, characterization and acid-base properties of kaolinite and metal (Fe, Mn, Co) doped kaolinite. *Appl. Clay Sci.* **179**, 105138 (2019).
99. Wu, C., Wei, X., Liu, P., Tan, J., Liao, C., Wang, H., Yin, L., Zhou, W., Cui, H. Influence of structural Al species on Cd(II) capture by iron muscovite nanoparticles. *Chemosphere* **226**, 907–914 (2019).
100. Kalmakhanova, M. S., Massalimova, B. K., Tuesta, J. L. D. & Gomes, H. T. Novelty pillared clays for the removal of 4-nitrophenol by catalytic wet peroxide

oxidation. *Ser. Geol. Tech. Sci.* **3**, 12–19 (2018).

101. Liu, Y., Dong, C., Wei, H., Yuan, W. & Li, K. Adsorption of levofloxacin onto an iron-pillared montmorillonite (clay mineral): Kinetics, equilibrium and mechanism. *Appl. Clay Sci.* **118**, 301–307 (2015).
102. Kern, A. & Eysel, W. Germany: University Heidelberg. in *Mineralogisch-Petrograph* (1993).
103. Howard, E. & Tatge, E. Patterns, Chapter 2. in *Circular of the Bureau of Standards: Standard X-ray diffractions powder patterns* 3–84 (1966).
104. Bahranowski, K. [Ti,Zr]-pillared montmorillonite - A new quality with respect to Ti- and Zr-pillared clays. *Microporous Mesoporous Mater.* **202**, 155–164 (2015).
105. Avena, M. J. & De Pauli, C. P. Proton adsorption and electrokinetics of an Argentinean montmorillonite. *J. Colloid Interface Sci.* **202**, 195–204 (1998).
106. Arfaoui, S., Hamdi, N. & Frini-Srasra, N. Determination of point of zero charge of PILCS with single and mixed oxide pillars prepared from Tunisian-smectite. **50**, 447–454 (2012).
107. Mnasri, S., Hamdi, N., Frini-Srasra, N. & Srasra, E. Acid–base properties of pillared interlayered clays with single and mixed Zr–Al oxide pillars prepared from Tunisian-interstratified illite–smectite. *Arab. J. Chem.* **10**, 1175–1183 (2017).
108. Breen, C. & Last, P. M. Catalytic transformation of the gases evolved during the thermal decomposition of HDPE using acid-activated and pillared clays. *J. Mater. Chem.* **9**, 813–818 (1999).
109. Tomul, F. Influence of Synthesis Conditions on the Physicochemical Properties and Catalytic Activity of Fe/Cr-Pillared Bentonites. *J. Nanomater.* **2012**, 1–14 (2012).
110. Mnasri-Ghnimi, S. & Frini-Srasra, N. Catalytic wet peroxide oxidation of phenol over Ce-Zr-modified clays: Effect of the pillaring method. *Korean J. Chem. Eng.* **32**, 68–73 (2015).
111. Velichkova, F., Julcour-Lebigue, C., Koumanova, B. & Delmas, H. Heterogeneous Fenton oxidation of paracetamol using iron oxide (nano)particles. *J. Environ. Chem. Eng.* **1**, 1214–1222 (2013).
112. Alalm, M. G., Tawfik, A. & Ookawara, S. Degradation of four pharmaceuticals by solar photo-Fenton process: Kinetics and costs estimation. *J. Environ. Chem. Eng.* **3**, 46–51 (2015).

113. Trovó, A. G., Pupo Nogueira, R. F., Agüera, A., Fernandez-Alba, A. R. & Malato, S. Paracetamol degradation intermediates and toxicity during photo-Fenton treatment using different iron species. *Water Res.* **46**, 5374–5380 (2012).
114. Liu, C., Cai, W. & Liu, L. Hydrothermal carbonization synthesis of Al-pillared montmorillonite@carbon composites as high performing toluene adsorbents. *Appl. Clay Sci.* **162**, 113–120 (2018).
115. Barakan, S. & Aghazadeh, V. Synthesis and characterization of hierarchical porous clay heterostructure from Al, Fe -pillared nano-bentonite using microwave and ultrasonic techniques. *Microporous Mesoporous Mater.* **278**, 138–148 (2019).
116. Vellayan, K., González, B., Trujillano, R., Vicente, M. A. & Gil, A. Pd supported on Cu-doped Ti-pillared montmorillonite as catalyst for the Ullmann coupling reaction. *Appl. Clay Sci.* **160**, 126–131 (2018).
117. Auer, H. & Hofmann, H. Pillared clays: characterization of acidity and catalytic properties and comparison with some zeolites. *Appl. Catal. A, Gen.* **97**, 23–38 (1993).

ATTACHMENTS

8 ATTACHMENTS

8.1 HYSTERESIS LOOPS

8.1.1 *Calcined samples*

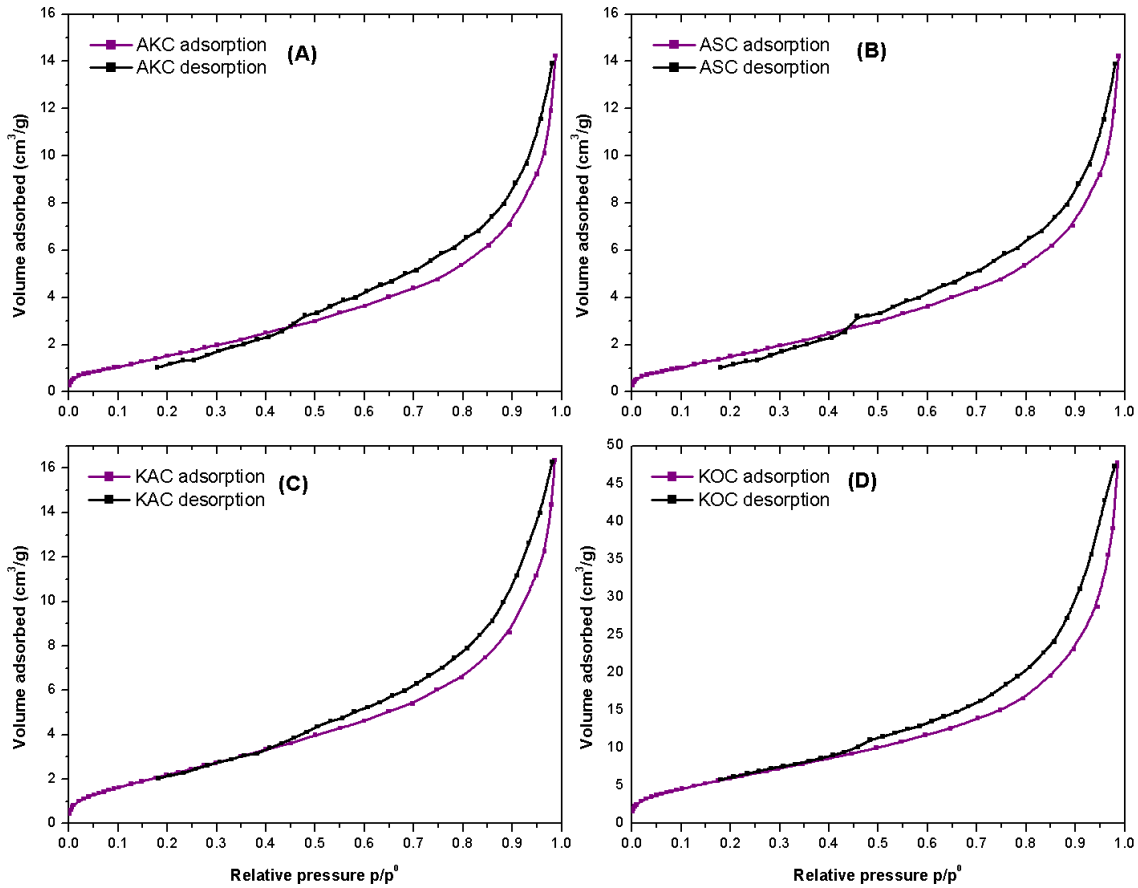

Figure 27. Hysteresis loop for calcined A) Akzhar, B) Asa, C) Karatau and D) Kokshetau.

8.1.2 *Natural samples*

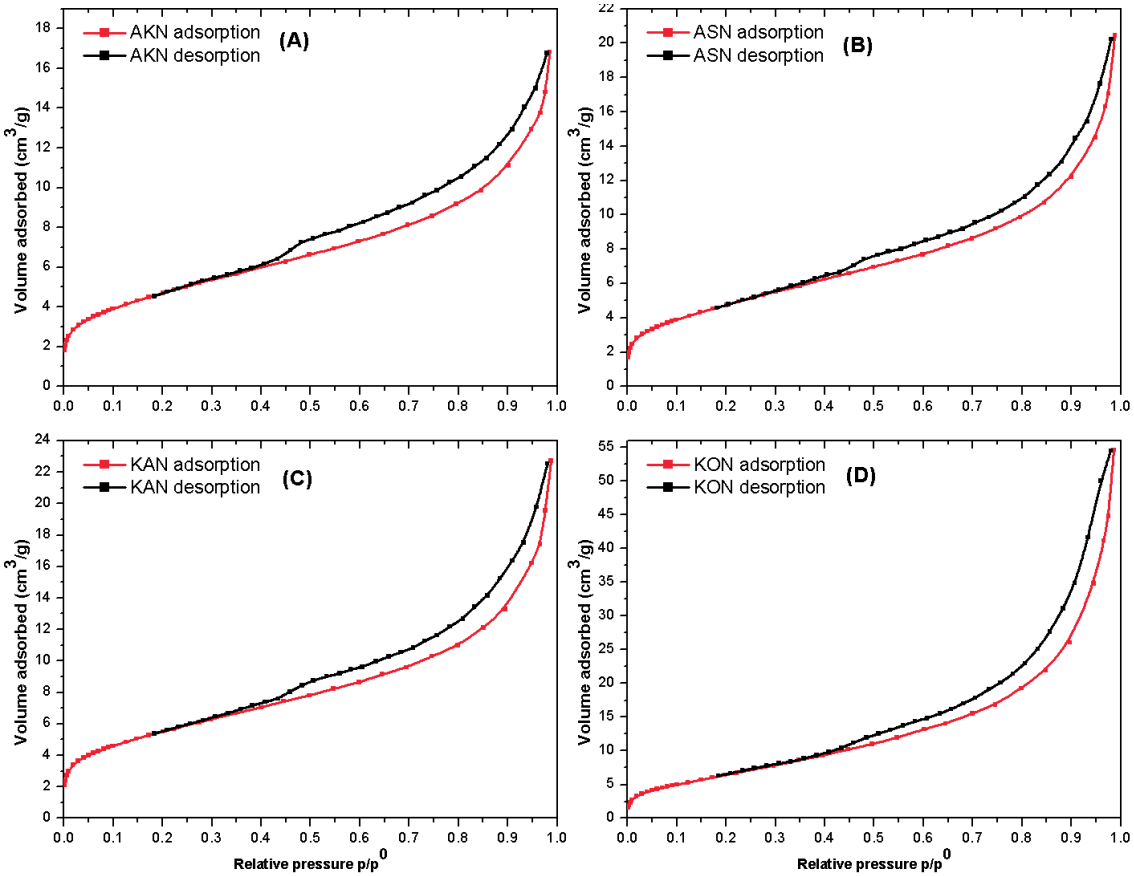

Figure 28. Hysteresis loop for natural A) Akzhar, B) Asa, C) Karatau and D) Kokshetau.

8.1.3 *Pillared samples*

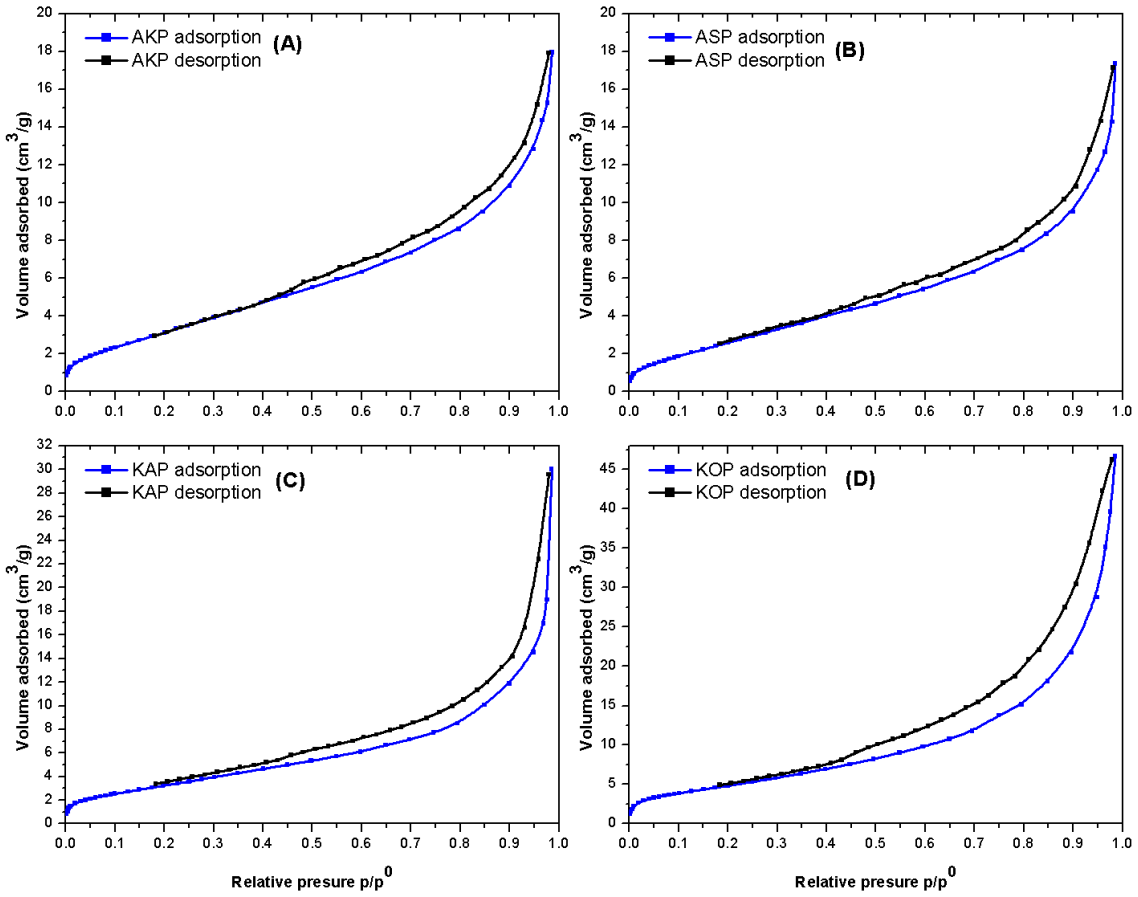

Figure 29. Hysteresis loop for pillared A) Akzhar, B) Asa, C) Karatau and D) Kokshetau.